

1 **Greenhouse gases emissions from riparian wetlands: An example from the**  
2 **Inner Mongolia grassland region in China**

3 **Xinyu Liu<sup>1,2</sup>, Xixi Lu<sup>1,3</sup>, Ruihong Yu<sup>1,2</sup>, Heyang Sun<sup>1</sup>, Hao Xue<sup>1</sup>, Zhen Qi<sup>1</sup>,**  
4 **Zhengxu Cao<sup>1</sup>, Zhuangzhuang Zhang<sup>1</sup>, Tingxi Liu<sup>4</sup>**

5 <sup>1</sup>Inner Mongolia Key Laboratory of River and Lake Ecology, School of Ecology and Environment,  
6 Inner Mongolia University, Hohhot 010021, China;

7 <sup>2</sup>Key Laboratory of Mongolian Plateau Ecology and Resource Utilization, Ministry of Education,  
8 Hohhot 010021, China;

9 <sup>3</sup>Department of Geography, National University of Singapore, 117570, Singapor;

10 <sup>4</sup>Inner Mongolia Water Resource Protection and Utilization Key Laboratory, Water Conservancy  
11 and Civil Engineering College, Inner Mongolia Agricultural University, Hohhot 010021, China

12 **Corresponding author:** Ruihong Yu (rhyu@imu.edu.cn) and Tingxi Liu (txliu@imau.edu.cn)

13  
14 **Abstract:** Gradual riparian wetland drying is increasingly sensitive to global warming and  
15 contributes to climate change. Riparian wetlands play a significant role in regulating carbon and  
16 nitrogen cycles. In this study, we analyzed the emissions of carbon dioxide (CO<sub>2</sub>), methane (CH<sub>4</sub>),  
17 and nitrous oxide (N<sub>2</sub>O) from riparian wetlands in the Xilin River Basin to understand the role of  
18 these ecosystems in greenhouse gas (GHG) emissions. Moreover, the impact of the catchment  
19 hydrology and soil property variations on GHG emissions over time and space were evaluated.  
20 Our results demonstrate that riparian wetlands emit larger amounts of CO<sub>2</sub> (335–2790 mg·m<sup>-2</sup>·h<sup>-1</sup>  
21 in wet season and 72–387 mg·m<sup>-2</sup>·h<sup>-1</sup> in dry season) than CH<sub>4</sub> and N<sub>2</sub>O to the atmosphere due to  
22 high plant and soil respiration. The results also reveal clear seasonal variations and spatial patterns  
23 along the transects and in the longitudinal direction. N<sub>2</sub>O emissions showed a spatiotemporal  
24 pattern similar to that of CO<sub>2</sub> emissions. Near-stream sites were the only sources of CH<sub>4</sub>  
25 emissions, while the other sites served as sinks for these emissions. Soil moisture content and soil  
26 temperature were the essential factors controlling the GHG emissions, and abundant aboveground  
27 biomass promoted the CO<sub>2</sub>, CH<sub>4</sub>, and N<sub>2</sub>O emissions. Moreover, compared to different types of  
28 grasslands, riparian wetlands were the potential hotspots of GHG emissions in the Inner  
29 Mongolian region. Degradation of downstream wetlands has resulted in reducing the soil carbon  
30 pool by approximately 60%, reducing CO<sub>2</sub> emissions by approximately 35%, and converting the

删除[liuxinyu]: 1

删除[liuxinyu]: 2

删除[liuxinyu]: 1

删除[liuxinyu]: 3

删除[liuxinyu]:

删除[liuxinyu]: in

删除[liuxinyu]: , Key Laboratory of River and Lake in Inner  
Mongolia Autonomous Region

删除[liuxinyu]: Inner Mongolia Autonomous,

删除[liuxinyu]: 2

删除[liuxinyu]: 3

删除[liuxinyu]:

31 ~~wetland from a CH<sub>4</sub> and N<sub>2</sub>O source to a sink~~, Our study showed that anthropogenic activities  
32 have extensively changed the hydrological characteristics of the riparian wetlands and might  
33 accelerate carbon loss, which could further affect the GHG emissions.

删除[liuxinyu]:

34

35 **Key words:** Riparian wetlands, Grasslands, Greenhouse gas, Spatial-temporal distribution, Impact  
36 factor, Xilin River Basin

37

38

39

## 40 **1. Introduction**

41 With the increasing impacts of global warming, the change in the concentrations of  
42 greenhouse gases (GHGs) in the atmosphere is a source of concern in the scientific community  
43 (Cao et al., 2005). According to the World Meteorological Organization (WMO, 2018), the  
44 concentrations of carbon dioxide (CO<sub>2</sub>), methane (CH<sub>4</sub>), and nitrous oxide (N<sub>2</sub>O) have increased  
45 by 146%, 257%, and 122%, respectively, since 1750. Despite their lower atmospheric  
46 concentrations, CH<sub>4</sub> and N<sub>2</sub>O absorb infrared radiation approximately 28 and 265 times more  
47 effectively at centennial timescales than CO<sub>2</sub> (IPCC, 2013). On a global scale, CO<sub>2</sub>, CH<sub>4</sub>, and N<sub>2</sub>O  
48 contribute 87% to the GHG effect (Ferrón et al., 2007).

49 Wetlands are unique ecosystems that serve as transition zones between terrestrial and aquatic  
50 ecosystems. They play an important role in the global carbon cycle (Beger et al., 2010; Naiman  
51 and Decamps, 1997). Wetlands are sensitive to hydrological changes, particularly in the context of  
52 global climate change (Cheng and Huang, 2016). Moreover, wetland hydrology is affected by  
53 local anthropogenic activities, such as the construction of reservoirs, resulting in gradual drying.  
54 Although wetlands cover only 4–6% of the terrestrial land surface, they contain approximately  
55 12–24% of global terrestrial soil organic carbon (SOC), thus acting as carbon sinks. Moreover,  
56 they release CO<sub>2</sub>, CH<sub>4</sub>, and N<sub>2</sub>O into the atmosphere and serve as carbon sources (Lv et al., 2013).

57 ~~In general, the carbon accumulation by plant's photosynthesis is higher than the consumption~~  
58 ~~(plant respiration, animal respiration, and microbial decomposition) in the wetland, thus the net~~  
59 ~~effect of the wetland is acted as a carbon sink~~, Wetlands are increasingly recognized as an  
60 essential part of nature, given their simultaneous functions as carbon sources and sinks. Excessive

删除[liuxinyu]: In general, plants' photosynthesis intensity is higher than respiration and decomposition in the wetland, thus the net effect of the wetland is acted as a carbon sink

61 rainfall will cause an expansion in wetland areas and a sharp increase in the soil moisture content,  
62 thus enhancing respiration, methanogenesis, nitrification, and denitrification rates (Mitsch et al.,  
63 2009). On the contrary, reduced precipitation or severe droughts will result in a decrease in water  
64 levels, causing the wetlands to dry up. The accumulated carbon will be released back into the  
65 atmosphere through oxidation. Due to the increasing impact of climate change and human activity,  
66 the drying of wetlands has been widely observed in recent years (Liu et al., 2006); more than half  
67 of global wetlands have disappeared since 1900 (Mitsch and Gosselink, 2007), and this tendency  
68 is expected to continue in the future. The loss of wetlands may directly shift the soil environment  
69 from anoxic to oxic conditions, and modify the CO<sub>2</sub> and CH<sub>4</sub> source and sink functions of wetland  
70 ecological systems (Waddington and Roulet, 2000; Zona et al., 2013).

71 The Xilin River Basin in China is characterized by a marked spatial gradient in soil moisture  
72 content. It is a unique natural laboratory that may be used to explore the close relationships  
73 between the spatiotemporal variations in hydrology and riparian biogeochemistry. Wetlands  
74 around the Xilin River play an irreplaceable role with regard to local climate control, water  
75 conservation, the carbon and nitrogen cycles, and husbandry (Gou et al., 2015; Kou, 2018).  
76 Moreover, the Xilin River region is subjected to seasonal alterations in precipitation and  
77 temperature regimes, and construction of the Xilin River Reservoir has resulted in highly negative  
78 consequences, such as the drying of downstream wetlands, affecting riparian hydrology as well as  
79 microbial activity in riparian soils. GHG emissions in riparian wetlands vary immensely.  
80 Understanding the interactions between GHG emissions and hydrological changes in the Xilin  
81 River riparian wetlands has thus become increasingly important. Moreover, it is necessary to  
82 estimate the changes in GHG emissions as a result of wetland degradation at local and global  
83 scales.

84 In this work, GHG emissions from riparian wetlands and adjacent hillslope grasslands of the  
85 Xilin River Basin were investigated. GHG emissions, soil temperature, and soil moisture content  
86 were measured in dry and wet seasons. The main objectives of this study were to (1) investigate  
87 the temporal and spatial variations in CO<sub>2</sub>, CH<sub>4</sub>, and N<sub>2</sub>O emissions from the wetlands in the  
88 riparian zone, and examine the main factors affecting the GHG emissions, (2) compare the GHG  
89 emissions from the riparian wetlands and different types of grasslands, and (3) evaluate the impact  
90 of wetland degradation in the study area on GHG emissions.

91

## 92 **2. Materials and methods**

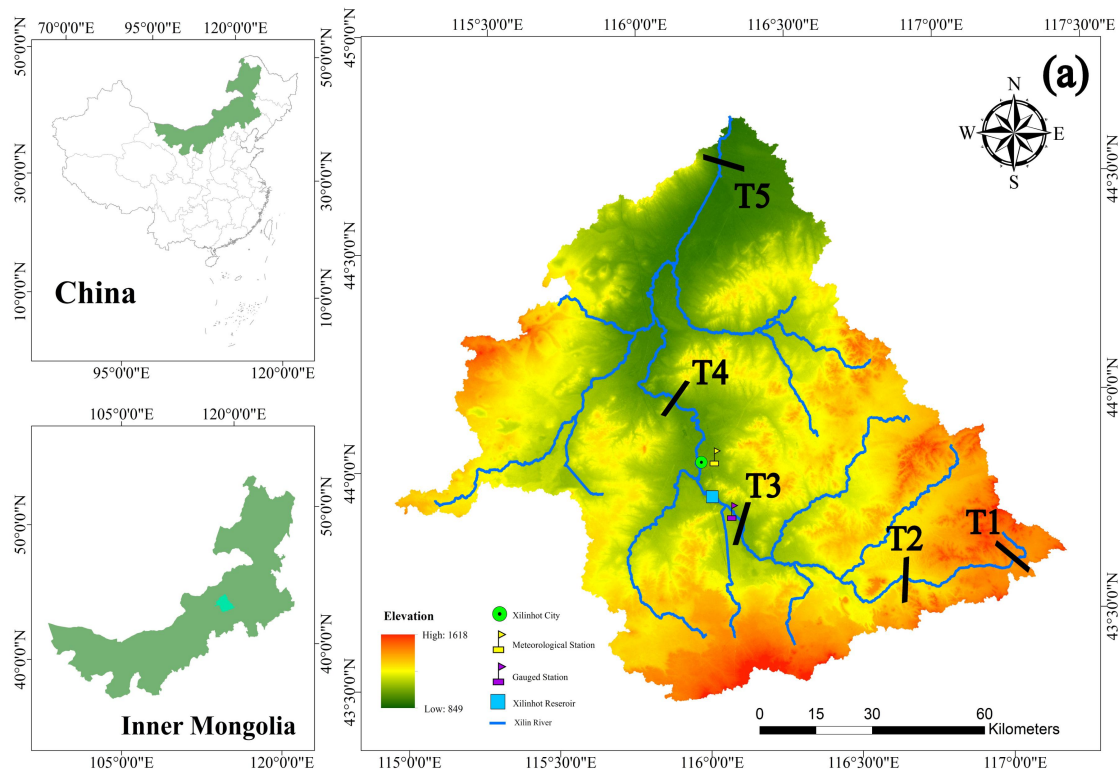
### 93 **2.1 Study site**

94 The Xilin River is situated in the southeastern part of the Inner Mongolia Autonomous  
95 Region in China (E115°00'–117°30', N43°26'–44°39'). It is a typical inland river of the Inner  
96 Mongolia grasslands. The river basin area is 10,542 km<sup>2</sup>, the total length is 268.1 km, and the  
97 average altitude is 988.5 m. According to the meteorological data provided by the Xilinhot  
98 Meteorological Station (Xi et al., 2017; Tong et al., 2004), the long-term annual mean air  
99 temperature is 1.7°C, and the maximum and minimum monthly means are 20.8°C in July and  
100 –19.8°C in January, respectively. The average annual precipitation was 278.9 mm for the period of  
101 1968–2015. Precipitation is distributed unevenly among the seasons, with 87.41% occurring  
102 between May and September.

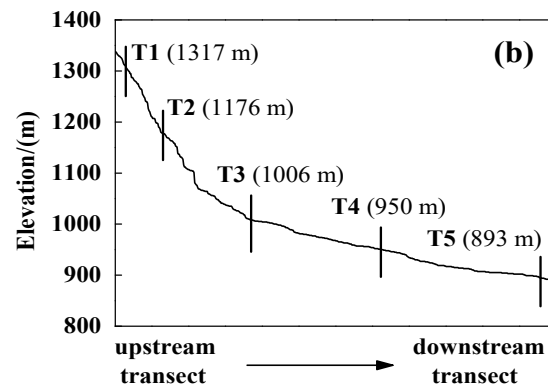
103 Soil types in the Xilin River Basin are predominantly chernozems (86.4%), showing a  
104 significant zonal distribution as light chestnut soil, dark chestnut soil, and chernozems from the  
105 northwest to southeast. Soil types in this basin also present a vertical distribution with elevation.  
106 The chernozems are primarily soluble chernozems and carbonate chernozems, distributed at  
107 altitudes above 1350 m with a relatively fertile and deep soil layer. Dark chestnut soil, boggy soil,  
108 and dark meadow with high humus content are distributed between the altitudes of 1150 and 1350  
109 m. Light chestnut soil, saline meadow soil, and meadow solonchak with low soil humus, a thin  
110 soil layer, and coarse soil texture are distributed between the altitudes of 902 and 1150 m (Xi et al.,  
111 2017).

### 112 **2.2 Field measurements and laboratory analyses**

113 In this study, five representative transects were selected as the primary measurement sites in  
114 the entire Xilin River. Each transect cuts through the riparian wetlands near the river and hillslope  
115 grasslands further away from it (Fig. 1).



116



117

118 Fig. 1 (a) Location of the Xilin River Basin and distribution of five riparian-hillslope transects

119 (T1–T5). (b) Elevation details of each transect in the Xilin River Basin.

120

121 The layout of the sampling points of each transect is shown in Fig. 2. Each sampling point

122 from T1–T5 was extended from the river to both sides, to the grassland on the slopes, using 5–7

123 sampling points for each transect and resulting in 24 points in total. The sampling sites on the left

124 and right banks were defined as L1–L3 and R1–R4 from the riparian wetlands to the hillslope

125 grasslands. As transect T3 was located on a much wider flood plain, none of its sampling points

126 were located on the hillslope grassland. The last transect (T5) was located downstream in the dry

127 lake and contained seven sampling points. They were defined as S1–S7, where S1, S2, and S7

128 were located along the lake shore (the lakeside zone), and S3–S6 were located in the dry lake bed  
129 (S3 and S4 in the mudbank, S5 in saline–alkali soil, and S6 in sand–gravel geology). Moreover,  
130 characterizations for T1, T2, and T3 transects were the continuous river flow and T4 and T5  
131 transects were the intermittent river flow.

132 The CO<sub>2</sub>, CH<sub>4</sub>, and N<sub>2</sub>O emissions from each site were measured in August (wet season) and  
133 October (dry season) in 2018 using a static dark chamber and the gas chromatography method.  
134 The static chambers were made of a cube-shaped polyvinyl chloride (PVC) pipe (dimensions: 0.4  
135 m × 0.2 m × 0.2 m). A battery-driven fan was installed horizontally inside the top wall of the  
136 chamber to ensure proper air mixing during measurements. To minimize heating from solar  
137 radiation, white adiabatic aluminum foil was used to cover the entire aboveground portion of the  
138 chamber. During measurements, the chambers were driven into the soil to ensure airtightness and  
139 connected with a differential gas analyzer (Li-7000 CO<sub>2</sub>/H<sub>2</sub>O analyzer, LI-COR, USA) to measure  
140 the changes in the soil CO<sub>2</sub> concentration. The air in the chamber was sampled using a 60 mL  
141 syringe at 0, 7, 14, 21, and 28 min. The gas samples were stored in a reservoir bag and taken to the  
142 laboratory for CH<sub>4</sub> and N<sub>2</sub>O measurements using gas chromatography (GC-2030, Japan). The  
143 measurements were scheduled for 9:00–11:00 a.m. or 3:00–5:00 p.m.

144 Soil temperature (ST) was measured at depths of 0–10 cm and 10–20 cm with a  
145 geothermometer (DTM-461, Hengshui, China). Plant samples were collected in a static chamber  
146 and oven-dried in the laboratory to obtain aboveground biomass (BIO). A 100 cm<sup>3</sup> ring cutter was  
147 used to collect surface soil samples at each site, which were placed in aluminum boxes and  
148 immediately brought back to the laboratory to measure soil mass moisture content (SMC) and soil  
149 bulk density ( $\rho_b$ ) using national standard methods (NATESC, 2006). Topsoil samples were  
150 collected, sealed in plastic bags, and brought back to the laboratory to measure soil pH, electrical  
151 conductivity (EC), total soil organic carbon (TOC), and soil C:N ratio.

152



153

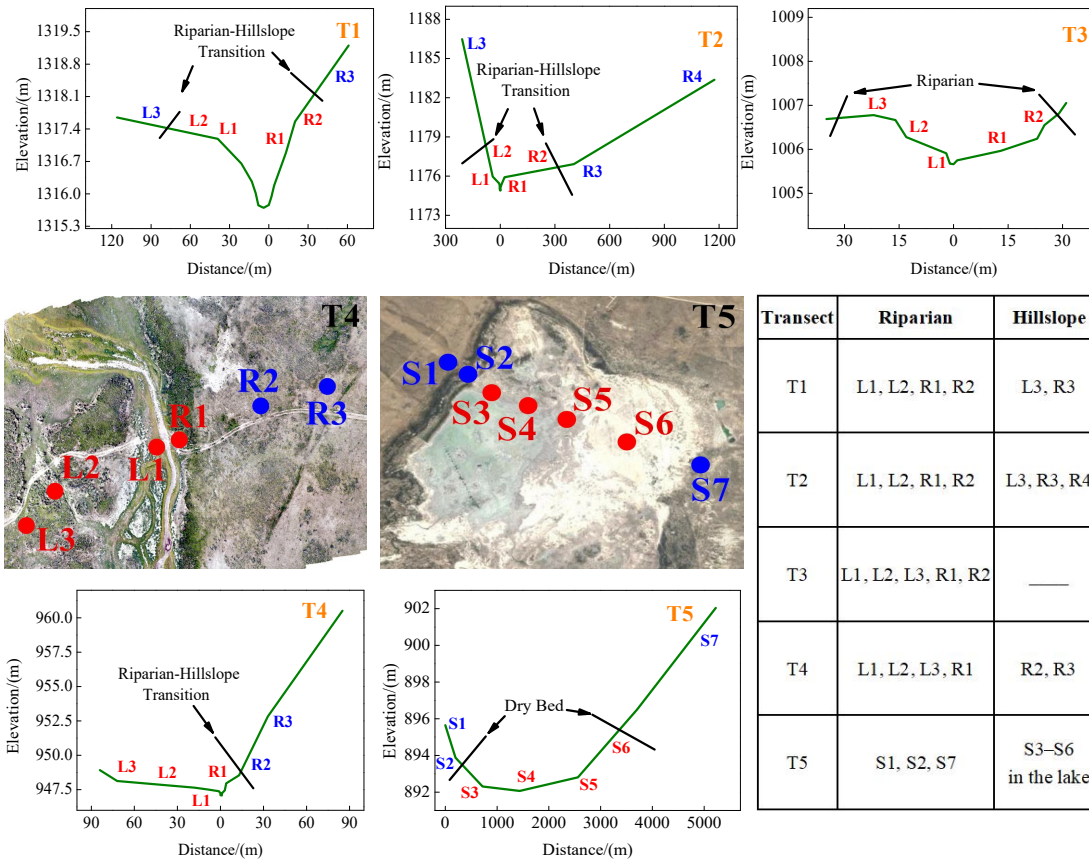


Fig. 2 Distributions of sampling points in transects T1–T5 (The images are authors' own)

Table 1. Physical and chemical properties (Mean  $\pm$  SD) of soils at various sites within each

transect

Trans ect	Zone	Sampl es numb er	transect								
			SMC10-V	SMC20-V	Soil C:N	TOC (g·kg <sup>-1</sup> )	BIO (g)	$\rho_b$	pH	EC ( $\mu$ s/cm)	SSM (%)
T1	Riparian	12	12.16 $\pm$ 7.55	12.88 $\pm$ 12.05	12.46 $\pm$ 0.91	30.16 $\pm$ 6.54	14.67 $\pm$ 5.44	1.28 $\pm$ 0.07	7.25 $\pm$ 0.62	154.71 $\pm$ 23.70	47.77 $\pm$ 7.04
	Hillslope	6	2.72 $\pm$ 0.91	5.05 $\pm$ 3.09	11.41 $\pm$ 0.09	10.77 $\pm$ 4.72	6.70 $\pm$ 1.48	1.45 $\pm$ 0.03	7.22 $\pm$ 0.40	82.02 $\pm$ 16.37	31.02 $\pm$ 1.32
T2	Riparian	12	26.75 $\pm$ 19.52	12.19 $\pm$ 7.82	11.70 $\pm$ 1.14	19.96 $\pm$ 5.71	24.76 $\pm$ 9.65	1.23 $\pm$ 0.05	8.95 $\pm$ 0.45	303.88 $\pm$ 102.16	51.21 $\pm$ 6.49
	Hillslope	9	5.85 $\pm$ 4.82	3.03 $\pm$ 1.43	9.77 $\pm$ 0.88	14.87 $\pm$ 11.21	6.10 $\pm$ 3.19	1.38 $\pm$ 0.13	8.10 $\pm$ 0.55	162.97 $\pm$ 128.18	35.09 $\pm$ 6.75
T3	Riparian	12	28.04 $\pm$ 22.95	14.53 $\pm$ 8.98	15.80 $\pm$ 4.16	22.40 $\pm$ 9.69	6.37 $\pm$ 2.95	1.35 $\pm$ 0.19	9.50 $\pm$ 0.67	1233.20 $\pm$ 829.83	47.56 $\pm$ 11.65
	L3	3	116.37 $\pm$ 113.36	113.36 $\pm$ 113.36	16.8 $\pm$ 16.8	36.1 $\pm$ 36.1	107.75 $\pm$ 107.75	0.592 $\pm$ 0.592	8.5 $\pm$ 8.5	403 $\pm$ 57.21	>100

			56.91	23.17	0.58	1.84	±16.94	0.02	0.17		
	Riparian	12	5.42 ± 3.34	4.07 ± 4.31	12.52 ± 2.06	9.96 ± 1.25	11.97 ± 4.50	1.30 ± 0.08	8.84 ± 0.22	461.72 ± 314.27	44.08 ± 7.07
T4	Hillslope	6	3.35 ± 2.06	4.27 ± 1.94	9.97 ± 0.50	9.65 ± 1.05	7.84 ± 2.48	1.30 ± 0.09	8.23 ± 0.14	118.5 ± 8.25	39.43 ± 5.55
	Dry lake bed	12	17.47 ± 15.08	14.49 ± 13.28	63.74 ± 12.93	31.41 ± 6.55	5.48 ± 2.35	1.16 ± 0.10	9.88 ± 0.18	7320.87 ± 4300.03	58.47 ± 7.16
T5	Lake shore	9	2.64 ± 1.48	2.82 ± 1.27	15.92 ± 4.71	6.35 ± 1.16	0	1.33 ± 0.09	9.41 ± 0.7	281.82 ± 162.73	37.52 ± 5.34

162 Note: SMC10-V - soil volumetric moisture content in 0-10 cm; SMC20-V -  
163 soil volumetric moisture content in 10-20 cm; Soil C:N - soil carbon-nitrogen ratio; TOC - total  
164 soil organic carbon; BIO - aboveground biomass;  $\rho_b$  - soil bulk density; pH - soil pH; EC - soil  
165 electrical conductivity; SSM - saturated soil moisture.

166

167 Table 2. soil particle composition of soils at various sites within each transect

Transect	Zone	soil particle composition		
		Clay % (<0.002 mm)	Silt % (0.02~0.002 mm)	Sand (2.0 ~0.02 mm)
T1	Riparian	2.5	2.7	94.8
	Hillslope	9.6	6.1	85.3
T2	Riparian	5.5	5.8	90.7
	Hillslope	10.8	8.6	80.6
T3	Riparian	4.1	1.1	94.8
T4	Riparian	11.4	1.5	87.1
	Hillslope	12.7	5.9	81.4
T5	Lake shore	5.1	2.1	92.8
	Dry lake bed	46.1	4.8	49.1

168

### 169 2.3 Calculation of GHG emissions

170 The CO<sub>2</sub>, CH<sub>4</sub>, and N<sub>2</sub>O emissions were calculated using Eq. 1 (Qin et al., 2016):

$$171 \quad F = \frac{V}{A} \times \frac{dc}{dt} \times \rho = H \times \frac{dc}{dt} \times \frac{M}{V} \times \left( \frac{273.15}{273.15 + t} \right) \quad (1)$$

172 Where  $F$  denotes the CO<sub>2</sub>, CH<sub>4</sub>, and N<sub>2</sub>O emissions (mg·m<sup>-2</sup>·h<sup>-1</sup>),  $H$  is the height of the static  
173 chamber (0.18 m),  $M$  is the relative molecular weight (44 for CO<sub>2</sub> and N<sub>2</sub>O, and 16 for CH<sub>4</sub>),  $V$  is  
174 the volume of gas in the standard state (22.4 L·mol<sup>-1</sup>),  $dc/dt$  is the rate of change of the gas  
175 concentration (10<sup>-6</sup>·h<sup>-1</sup>), and  $T$  is the temperature in the black chamber (°C).

176 The annual cumulative emissions were calculated using Eq. 2 (Whiting G and Chanton J.,  
177 2001)

$$178 \quad M = \sum \frac{F_{i+1} + F_i}{2} \times (t_{i+1} - t_i) \times 24 \quad (2)$$

179 Where M denotes the total cumulative emissions of CO<sub>2</sub>, CH<sub>4</sub>, or N<sub>2</sub>O (kg·hm<sup>2</sup>), F is the emission  
180 flux of CO<sub>2</sub>, CH<sub>4</sub>, or N<sub>2</sub>O, i is the sampling frequency, t<sub>i+1</sub>-t<sub>i</sub> represents the interval between two  
181 adjacent measurement dates.

182 In this study, a 100-year scale was selected to calculate the global warming potential (GWP)  
183 of soil CH<sub>4</sub> and N<sub>2</sub>O emissions (Whiting G and Chanton J., 2001):

$$184 \quad GWP = 1 \times [CO_2] + 25 \times [CH_4] + 298 \times [N_2O] \quad (3)$$

185 Where 25 and 298 are GWP multiples of CH<sub>4</sub> and N<sub>2</sub>O relative to CO<sub>2</sub> on a 100-year time scale,  
186 respectively.

## 187 **2.4 Statistical Analysis**

188 All statistical analyses were performed using SPSS for Windows version 18.0 (SPSS Inc.,  
189 Chicago, IL, USA). Statistical significance was set at P < 0.05. Pearson correlation analysis was  
190 conducted to estimate the relationships between GHGs fluxes and environmental variables. A  
191 Wilcoxon test was used to determine the difference of GHGs fluxes in two seasons.

## 192 **3. Results**

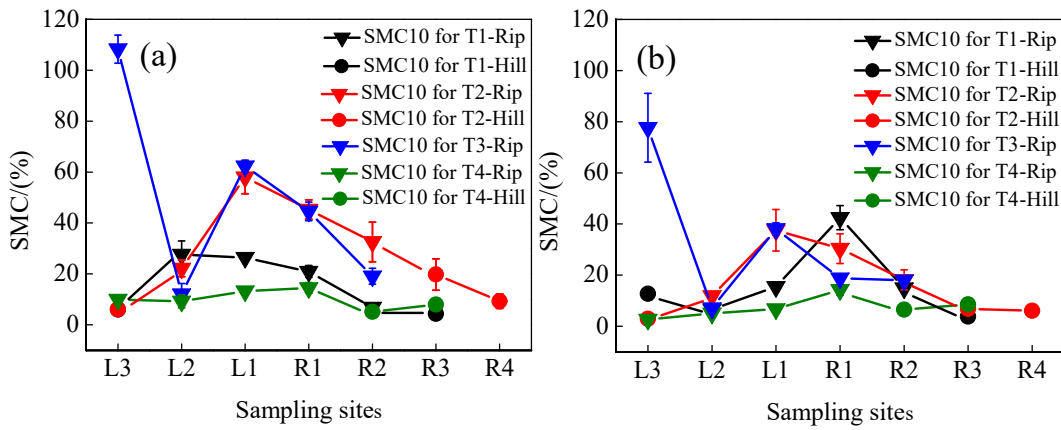
### 193 **3.1 Spatiotemporal patterns of SMC for each transect**

194 The temporal and spatial variations in SMC10 in the following order: wet season > dry  
195 season and riparian wetlands > hillslope grasslands (Fig. 3a, c, e). Similar variations were  
196 observed in SMC20 (Fig. 3b, d, f). The average SMC10 and SMC20 in the continuous river  
197 transects in the riparian zones (37.44% in wet season and 19.40% in dry season; 25.96% in wet  
198 season and 17.39% in dry season) were higher than those in the hillslope grasslands (9.12% in wet  
199 season and 4.15% in dry season; 6.51% in wet season and 5.96% in dry season). During the study  
200 period, both SMC10 and SMC20 changed as the distance from the river increased, and the highest  
201 value was observed at the near-stream sites (L1 and R1). SMC10 fluctuations were low in the  
202 intermittent transect compared to the upstream transects, with a mean value of 11.79% in wet  
203 season and 3.72% in dry season in the riparian areas. The mean SMC10 in the hillslopes was

204 6.58% in wet season and 2.86% in dry season. SMC20 showed similar fluctuation, 7.22% in wet  
 205 season and 2.98% in dry season in the riparian areas and 7.56% in wet season and 4.4% in dry  
 206 season in the hillslopes. In transect T5, average SMC10 and SMC20 at the center of the lake  
 207 (29.00% in wet season and 13.36% in dry season; 29.30% in wet season and 9.69% in dry season)  
 208 were higher than those along the lake shore (4.90% in wet season and 3.13% in dry season; 3.34%  
 209 in wet season and 5.22% in dry season).

210

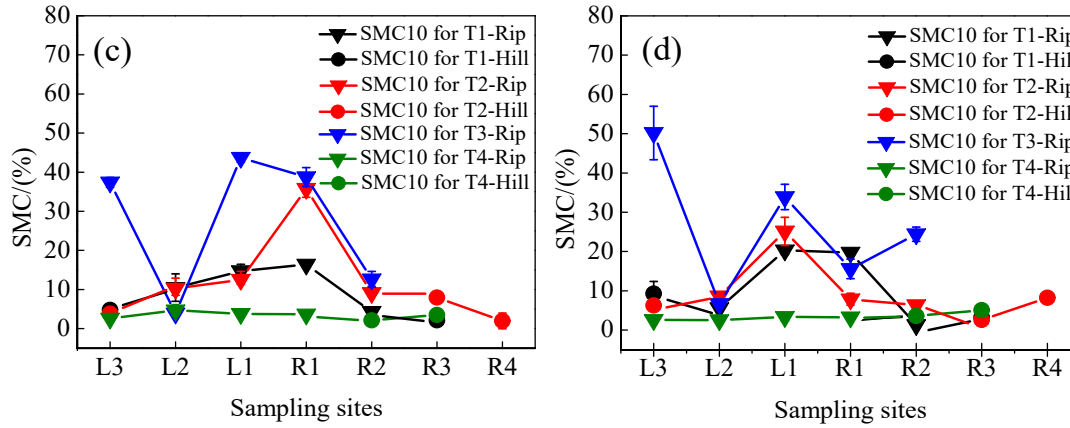
Wet season



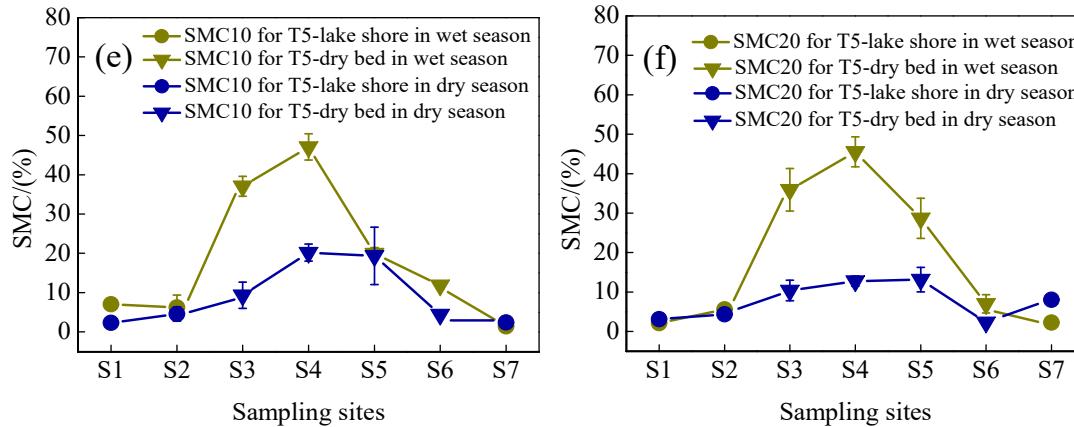
211

212

Dry season



213



214

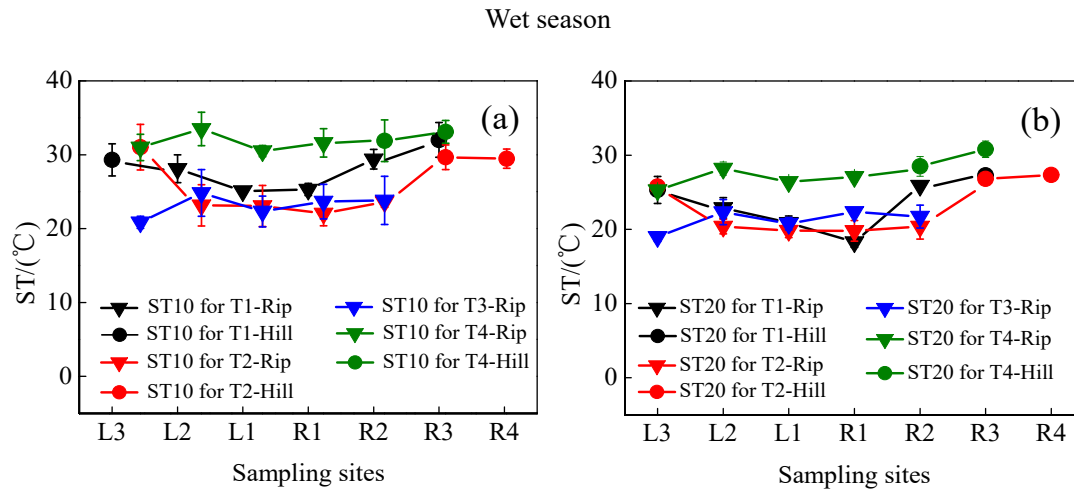
215

216 Fig. 3 Soil mass moisture contents (SMCs) at soil depths of 0–10 cm (SMC10) and 10–20 cm  
217 (SMC20) for transects T1–T5 in wet season and dry season. Error bars represent the SD about the  
218 mean.  
219

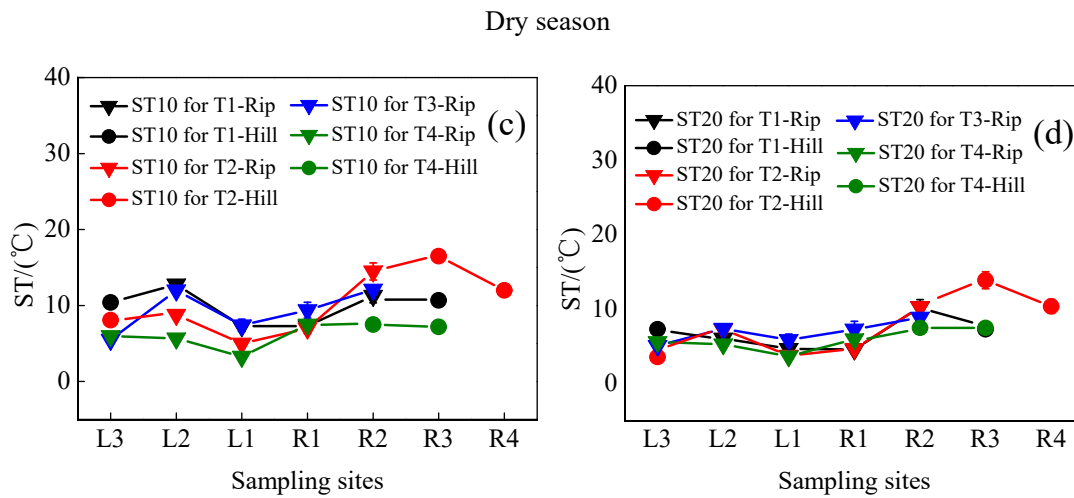
### 220 3.2 Spatiotemporal patterns of ST in each transect

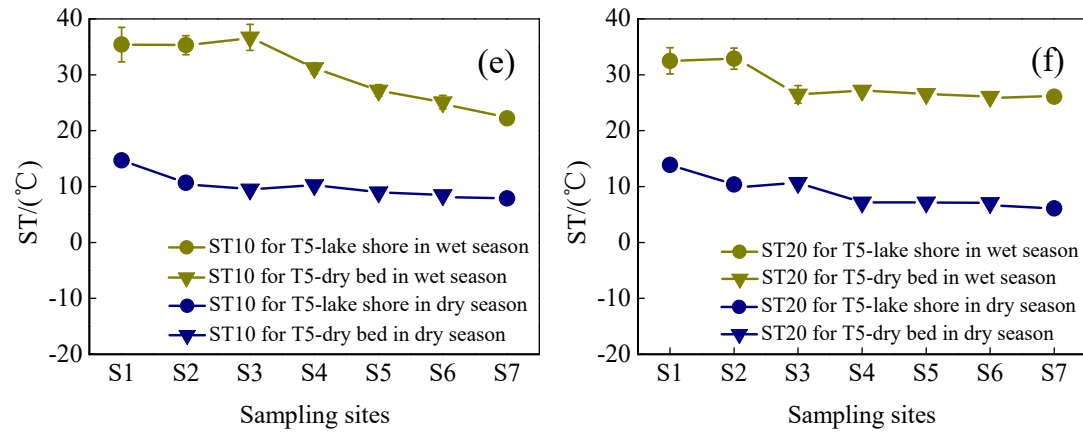
221 Spatiotemporal differences in ST during the entire observation period are displayed in Fig. 4.  
222 ST variations in wet season (mean value: 27.4°C) were noticeably higher than those in dry season  
223 (mean value: 8.97°C). Moreover, ST for riparian sites (mean values: 26.0°C in wet season and  
224 8.41°C in dry season) was slightly lower than that for the hillslope grasslands (mean values:  
225 30.9°C in wet season and 10.3°C in dry season) for the 0–10 cm soil depth, with the exception of  
226 transect T5. Similar results were observed for the 10–20 cm soil depth.

227



229





231

232 Fig. 4 Soil temperatures (STs) at soil depths of 0–10 cm (ST10) and 10–20 cm (ST20) for

233 transects T1–T5 in wet season and dry season. Error bars represent the SD about the mean.

234

### 235 3.3 Spatiotemporal patterns of GHG emissions in each transect

236 Figure 5 shows the spatiotemporal variations in GHG emissions in wet season and dry season

237 in each transect. CO<sub>2</sub> emissions in each transect were higher in wet season than in dry season. The

238 average emissions for the riparian wetlands of transects T1–T4 ( $1582.09 \pm 679.34 \text{ mg}\cdot\text{m}^{-2}\cdot\text{h}^{-1}$  in

239 wet season and  $163.24 \pm 84.98 \text{ mg}\cdot\text{m}^{-2}\cdot\text{h}^{-1}$  in dry season) were higher than those for the hillslope

240 grasslands ( $1071.54 \pm 225.39 \text{ mg}\cdot\text{m}^{-2}\cdot\text{h}^{-1}$  in wet season and  $77.68 \pm 25.32 \text{ mg}\cdot\text{m}^{-2}\cdot\text{h}^{-1}$  in dry

241 season). Higher CO<sub>2</sub> fluxes occurred in the riparian zones, while lower CO<sub>2</sub> fluxes were observed

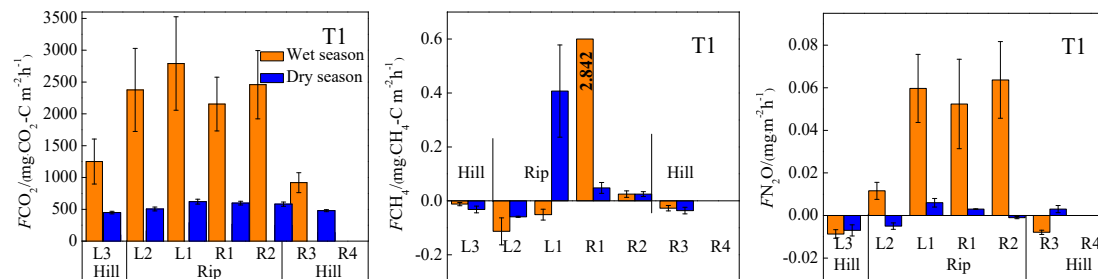
242 in the hillslope grasslands in continuous river transects (T1, T2, and T3). Transect T4 exhibited

243 lower CO<sub>2</sub> emissions in the riparian wetlands near the channel than at sites away from the channel.

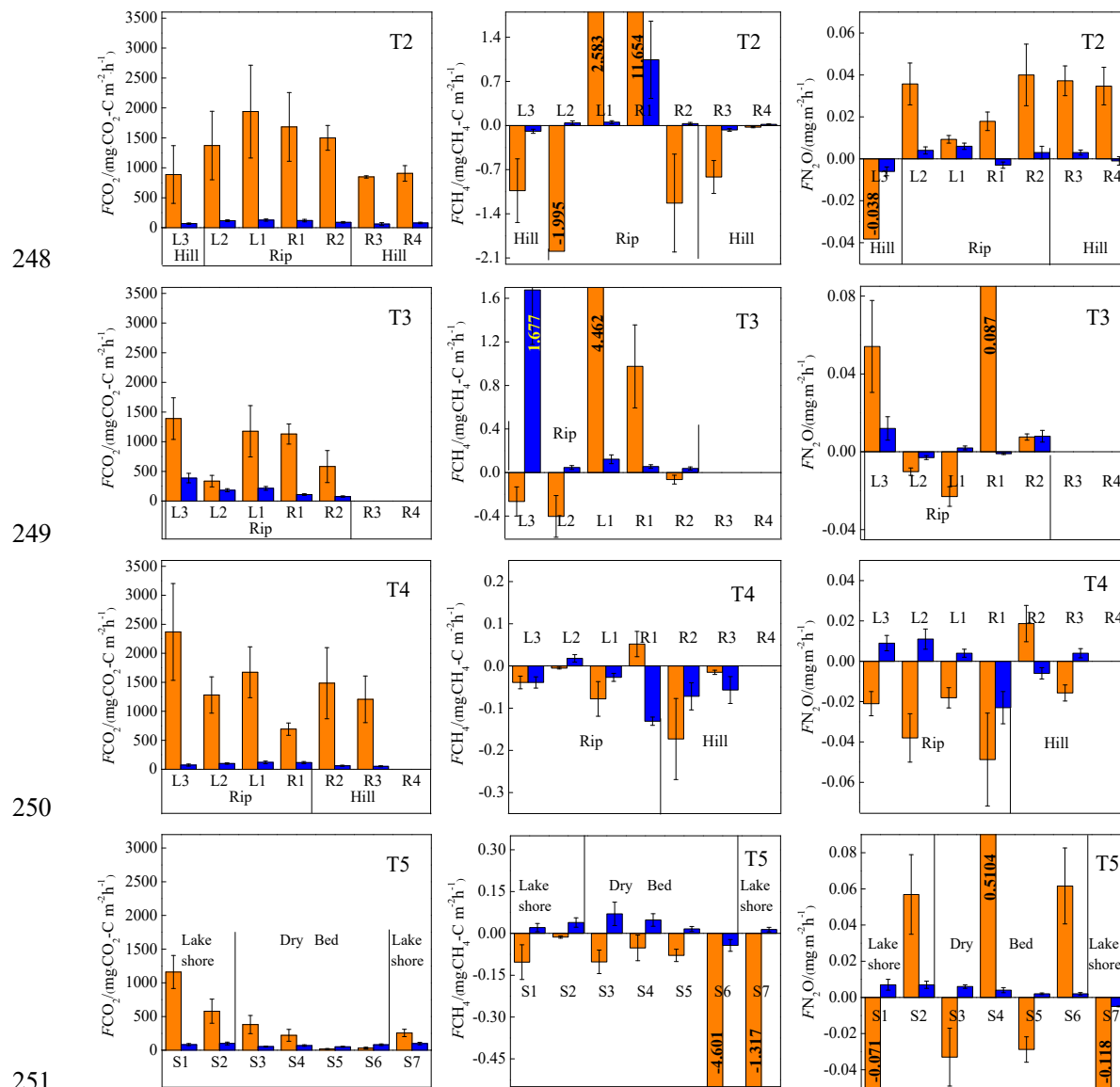
244 CO<sub>2</sub> emissions in transect T5 in wet season and dry season decreased from the lake shore to the

245 lake center.

246



247



248

249

250

251

252 Fig. 5 Spatiotemporal patterns of CO<sub>2</sub> (first column), CH<sub>4</sub> (second column), and N<sub>2</sub>O  
 253 (third column) emissions ( $F$ ) for each transect. Data are shown for wet season (orange) and dry  
 254 season (blue) and error bars are the standard deviations.

255

256 CH<sub>4</sub> emissions at the transects with continuous river flow (T1, T2, and T3) varied between  
 257 wet season and dry season, except for T4 (characterized by intermittent river flow) and T5 (the dry  
 258 lake). In wet season, the near-stream sites (L1 and R1) in T1, T2, and T3 were characterized as  
 259 high CH<sub>4</sub> sources (average:  $3.74 \pm 3.81 \text{ mg} \cdot \text{m}^{-2} \cdot \text{h}^{-1}$ ), but the sites located away from the river  
 260 gradually turned into CH<sub>4</sub> sinks. Moreover, all the sites in transects T4 and T5 were sinks. CH<sub>4</sub>  
 261 emissions (mean value:  $0.2 \pm 0.45 \text{ mg} \cdot \text{m}^{-2} \cdot \text{h}^{-1}$ ) at the wetland sites were always lower in dry  
 262 season than those in wet season. However, the sites on the hillslope grasslands served as CH<sub>4</sub>

263 sinks (mean value:  $-0.05 \pm 0.03 \text{ mg} \cdot \text{m}^{-2} \cdot \text{h}^{-1}$ ). In transect T5, CH<sub>4</sub> emissions revealed the opposite  
 264 trend; a CH<sub>4</sub> sink was observed in wet season, but it was transformed into a CH<sub>4</sub> source in dry  
 265 season.

266 Similar to the CO<sub>2</sub> and CH<sub>4</sub> emissions, N<sub>2</sub>O emissions showed a distinct spatiotemporal  
 267 pattern for all the transects. N<sub>2</sub>O emissions in wet season were higher than those in dry season.  
 268 These emissions were higher in riparian wetlands than in hillslope grasslands. Moreover, almost  
 269 all the sites with continuous river flow were N<sub>2</sub>O sources, while more than half of the sites with  
 270 intermittent river flow were sinks.

271 Table 3 shows that CO<sub>2</sub> fluxes were significantly correlated between the wet season and dry  
 272 season, while CH<sub>4</sub> and N<sub>2</sub>O fluxes were not correlated in two seasons.

273 Table 3 Significant correlations between GHGs fluxes and two seasons (n=31)

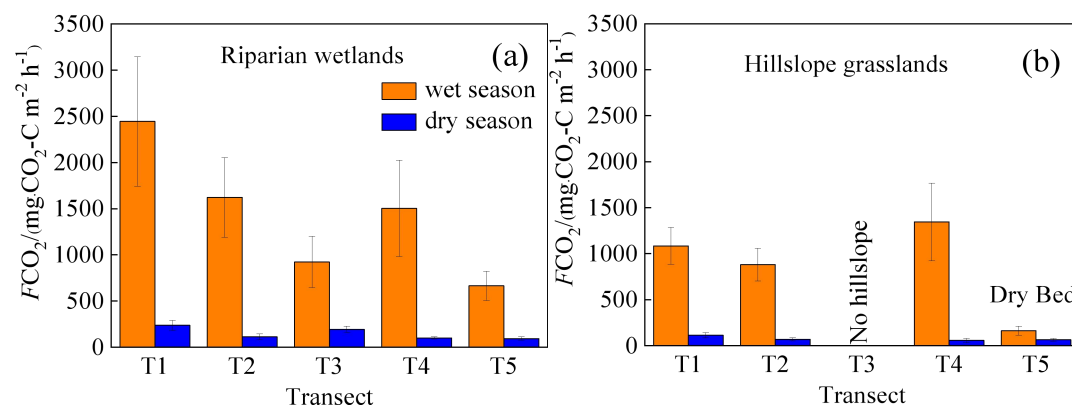
GHG flux	FCO <sub>2</sub> in wet season-FCO <sub>2</sub> in dry	FCH <sub>4</sub> in wet season-FCH <sub>4</sub> in dry	FN <sub>2</sub> O in wet season- FN <sub>2</sub> O in dry
	season	season	season
significant correlations (P)	0.000	0.133	0.290

274 Note: P<0.05 denote significant correlations and P > 0.05 denote no significant correlations

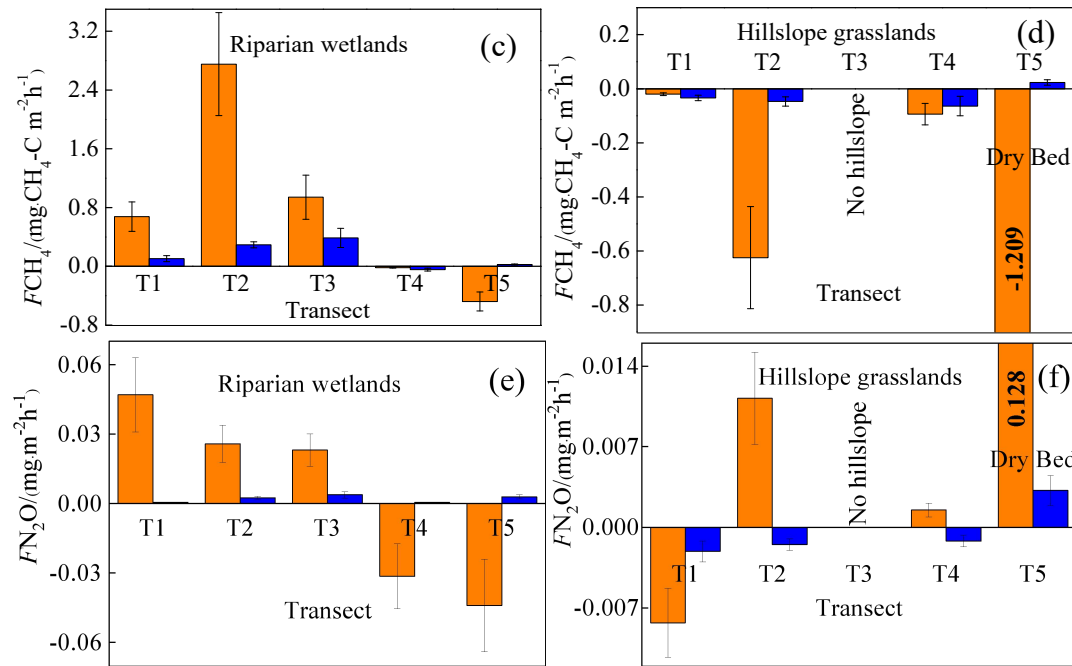
### 275 3.4 Spatiotemporal patterns of GHG emissions in upstream and downstream 276 areas

277 Figure 6 shows the detailed spatial and seasonal distribution of GHG emissions in wet season  
 278 and dry season in the longitudinal direction from the upstream (T1, T2, and T3) to the downstream  
 279 areas (T4 and T5). The CO<sub>2</sub>, CH<sub>4</sub>, and N<sub>2</sub>O emissions were calculated from the average values of  
 280 the respective emissions in the wetlands and hillslope grasslands in each transect.

281



282



283

284

285 Fig. 6 Spatiotemporal patterns of CO<sub>2</sub> (first line), CH<sub>4</sub> (second line), and N<sub>2</sub>O (third line)

286 emissions ( $F$ ) in the upstream (T1, T2, and T3) and downstream areas (T4 and T5). Bars are the

287 mean values for each transect and error bars are the standard errors.

288

289 CO<sub>2</sub> emissions in riparian wetlands (Fig. 6(a)) in wet season decreased from  $2444.69 \pm$   
 290  $228.58 \text{ mg}\cdot\text{m}^{-2}\cdot\text{h}^{-1}$  in the upstream area to  $665.08 \pm 347.57 \text{ mg}\cdot\text{m}^{-2}\cdot\text{h}^{-1}$  downstream, and the  
 291 corresponding values for dry season were  $238.12 \pm 48.20 \text{ mg}\cdot\text{m}^{-2}\cdot\text{h}^{-1}$  and  $94.14 \pm 7.67$   
 292  $\text{mg}\cdot\text{m}^{-2}\cdot\text{h}^{-1}$ . However, in hillslope grasslands (Fig. 6(b)), CO<sub>2</sub> emissions exhibited no significant  
 293 seasonality between upstream and downstream areas, with the mean values of  $1103.40 \pm 190.44$   
 294  $\text{mg}\cdot\text{m}^{-2}\cdot\text{h}^{-1}$  in wet season and  $79.18 \pm 24.52 \text{ mg}\cdot\text{m}^{-2}\cdot\text{h}^{-1}$  in dry season. In addition, CO<sub>2</sub> emissions  
 295 in transect T5 were lower for both months, with the averages of  $162.83 \pm 149.15 \text{ mg}\cdot\text{m}^{-2}\cdot\text{h}^{-1}$  and  
 296  $63.26 \pm 12.40 \text{ mg}\cdot\text{m}^{-2}\cdot\text{h}^{-1}$  in wet season and dry season, respectively. The upstream riparian zones  
 297 exhibited higher CO<sub>2</sub> emissions ( $894.32 \pm 868.47 \text{ mg}\cdot\text{m}^{-2}\cdot\text{h}^{-1}$ ) than their downstream counterparts  
 298 ( $621.14 \pm 704.10 \text{ mg}\cdot\text{m}^{-2}\cdot\text{h}^{-1}$ ). However, mean CO<sub>2</sub> emissions showed no significant differences  
 299 in grasslands, averaging  $524.16 \pm 450.10 \text{ mg}\cdot\text{m}^{-2}\cdot\text{h}^{-1}$  upstream and  $508.06 \pm 534.77 \text{ mg}\cdot\text{m}^{-2}\cdot\text{h}^{-1}$   
 300 downstream.

301 CH<sub>4</sub> emissions showed a marked spatial pattern in the riparian zones from upstream to  
 302 downstream (Fig. 6(c)). The transects with continuous river flow were CH<sub>4</sub> sources in wet season  
 303 and dry season, with the average emissions of  $1.42 \pm 3.41 \text{ mg}\cdot\text{m}^{-2}\cdot\text{h}^{-1}$  and  $0.27 \pm 0.49 \text{ mg}\cdot\text{m}^{-2}\cdot\text{h}^{-1}$ ,

304 respectively, while those with intermittent river flow served as CH<sub>4</sub> sinks, with the corresponding  
305 mean values of  $-0.21 \pm 0.45 \text{ mg}\cdot\text{m}^{-2}\cdot\text{h}^{-1}$  and  $-0.02 \pm 0.05 \text{ mg}\cdot\text{m}^{-2}\cdot\text{h}^{-1}$ . Moreover, the hillslope  
306 grassland sites in all transects were CH<sub>4</sub> sinks (Fig. 6(d)).

307 N<sub>2</sub>O emissions in riparian wetlands (Fig. 7(e)) showed spatial patterns similar to those of  
308 CH<sub>4</sub> emissions. In wet season, the transects with continuous river flow served as N<sub>2</sub>O sources,  
309 with the mean value of  $0.031 \pm 0.031 \text{ mg}\cdot\text{m}^{-2}\cdot\text{h}^{-1}$ , while those with intermittent river flow were  
310 N<sub>2</sub>O sinks with an average value of  $-0.037 \pm 0.05 \text{ mg}\cdot\text{m}^{-2}\cdot\text{h}^{-1}$ . In dry season, N<sub>2</sub>O emissions  
311 occurred as weak sources in the longitudinal transects, averaging  $0.002 \pm 0.007 \text{ mg}\cdot\text{m}^{-2}\cdot\text{h}^{-1}$ .  
312 However, N<sub>2</sub>O emissions in hillslope grasslands did not show any spatial pattern (Fig. 7(f)).

## 313 **4. Discussion**

### 314 **4.1 Main factors influencing GHG emissions**

#### 315 4.1.1 Effects of SMC on GHG emissions

316 SMC constituted one of the main factors affecting GHG emissions in wetlands. In this study,  
317 transects T1–T4 were characterized by a marked spatial SMC gradient (i.e., a gradual decrease  
318 include SMC10 and SMC20 from the riparian wetlands to the hillslope grasslands and from  
319 upstream to downstream (Fig. 3)). The CO<sub>2</sub>, CH<sub>4</sub>, and N<sub>2</sub>O emissions showed a similar trend. In  
320 Table 4, SMC10 is positive correlated with CO<sub>2</sub> emissions ( $P < 0.05$ ), SMC10 and SMC20 are  
321 significantly positive correlated with CH<sub>4</sub> emissions ( $P < 0.01$ ), and SMC10 and SMC20 are  
322 highly positive correlated with N<sub>2</sub>O emissions ( $P < 0.05$  and  $P < 0.01$ , respectively). These results  
323 indicated the influence of wetland SMC on GHG emissions.

324 Typically, the optimal SMC values associated with CO<sub>2</sub> emissions in riparian wetlands range  
325 from 40 to 60% (Sjögersten et al., 2006), creating better soil aeration and improving soil  
326 microorganisms' activity and the respiration of plant roots, thereby promoting CO<sub>2</sub> emissions,  
327 whereas excessive SMC reduces soil gas transfer due to the formation of an anaerobic  
328 environment in the soil, and microbial activity is lower, favoring the accumulation of organic  
329 matter (Hui., 2014). On the contrary, the SMC of hillslope grasslands is less than 10%. Low soil  
330 moisture inhibits the growth of vegetation with few vegetation residues and litters. Meanwhile,  
331 low soil moisture is not conducive to the survival of soil microorganisms, leading to a decrease in  
332 CO<sub>2</sub> emissions than to those in riparian zones (Moldrup et al., 2000; Hui., 2014). Similar results  
333 were obtained in our study. The changes in CO<sub>2</sub> emissions in transect T5 were contrary to the

334 change in the SMC10 and SMC20 likely because the optimal range of soil C:N is between 10-12  
335 (Pierzynski et al., 1994), but the value in the dry lake bed of T5 is higher than 60, high soil C:N  
336 resulted in nitrogen limitation in the process of decomposition of organic matter by  
337 microorganisms. Furtherly, other sediment properties (like Soil pH>9.5) for this transect were not  
338 conducive to the survival of microorganisms (Table 1), and the increase in SMC did not increase  
339 the respiration activity of microorganisms.

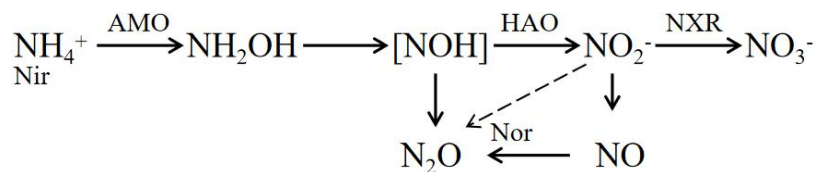
340 The largest CH<sub>4</sub> emissions were observed at the near-stream sites (i.e., L1 and R1) in T1, T2,  
341 and T3, with the average SMC of 30.29%, while the SMC values at the other sites, which were  
342 either weak sources or sinks, averaged at 14.57%. These results indicate that a higher SMC is  
343 favorable for CH<sub>4</sub> emissions because a higher SMC denotes a soil in a reduced state, which is  
344 beneficial for CH<sub>4</sub> production and inhibits CH<sub>4</sub> oxidation. A similar result was reported by Xu et al.  
345 (2008). They conducted experiments of CH<sub>4</sub> emissions from a variety of paddy soils in China, and  
346 showed that CH<sub>4</sub> production rates increased with the increase in SMC at the same incubation  
347 temperature. Meng et al. (2001) also reported that water depth was the main factor affecting CH<sub>4</sub>  
348 emissions from wetlands. When the water level dropped below the soil surface, the decomposition  
349 of organic matter accelerated, and CH<sub>4</sub> emissions decreased. If the oxide layer is large, the soil is  
350 transformed into a CH<sub>4</sub> sink (Meng et al., 2011).

351 The N<sub>2</sub>O fluxes showed a clear spatial pattern associated with the changes in SMC. The  
352 moisture content of wetland soils directly affects the aeration status of the soil. Besides, the  
353 aeration status affects the partial pressure of oxygen, which has an important impact on  
354 nitrifying/denitrifying bacteria's activity and ultimately affects soil N<sub>2</sub>O emissions (Zhang et al.,  
355 2005). Table 4 shows that N<sub>2</sub>O emissions are significantly positively correlated with SMC10 and  
356 SMC20 ( $P < 0.01$ ). Generally, when SMC was below the saturated water content, the  
357 microorganisms were in an aerobic environment, and N<sub>2</sub>O mainly came from the nitrification  
358 reaction. N<sub>2</sub>O emissions increases with the increase of SMC (Niu et al., 2017; Yu et al., 2006). In  
359 our study, the sampling sites with higher SMC (riparian zones and some hillslope grassland zones  
360 in the upstream transects) have higher N<sub>2</sub>O emissions. When SMC increases to the saturated water  
361 content or is in a flooded state, the system was an anaerobic environment, and the Nos activity  
362 was higher due to excessively high SMC, which was conducive to denitrification and eventually  
363 produced N<sub>2</sub> (Niu et al., 2017; Yu et al., 2006), such as site L1 in transect T3 in this study. Ulrike

364 et al. (2004) showed that denitrification was the main process under flooded soil conditions in  
 365 wetland soils, and the release of N<sub>2</sub> exceeds N<sub>2</sub>O. These findings are consistent with those of Liu  
 366 et al. (2003), who showed that SMC is an essential factor affecting N<sub>2</sub>O emissions.

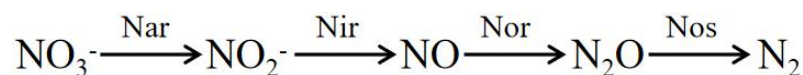
367

368 Nitrification:



369

370 Denitrification:



371

372 The enzymes involved in the formula include Ammonia monooxygenase (AMO),  
 373 Hydroxylamine oxidase (HAO), Nitrite REDOX enzyme (HAO), nitrate reductase (Nar), nitrite  
 374 reductase (Nir), Nitric oxide reductase (Nor) and Nitrous oxide reductase (Nos).

#### 375 4.1.2 Effects of ST on GHG emissions

376 ST was another important factor affecting the CO<sub>2</sub> emissions in this study, as this parameter  
 377 was significantly correlated with CO<sub>2</sub> emissions ( $P < 0.01$ ) (Table 4). The activity of soil  
 378 microorganisms increases with rising soil temperatures, leading to increased respiration, and  
 379 consequently higher CO<sub>2</sub> emissions (Heilman et al., 1999). Previous studies reported that ST  
 380 partially controls seasonal CO<sub>2</sub> emission patterns (Inubushi et al., 2003). Therefore, CO<sub>2</sub>  
 381 emissions in wet season were significantly higher than those in dry season in this study.

382 CH<sub>4</sub> emissions showed a clear seasonal pattern because high summer temperatures improve  
 383 the activity of both CH<sub>4</sub>-producing and -oxidizing bacteria (Ding et al., 2010). However, Table 4  
 384 indicates that the correlation between CH<sub>4</sub> emissions and temperature is not significant because  
 385 SMC could be more critical than temperature in our study region with very dry climate. SMC  
 386 showed a positive correlation with GHG emissions. In addition, SMC affected ST to a certain  
 387 extent, while the interactions between SMC and ST had a mutual influence on CH<sub>4</sub> emissions.  
 388 During the study period, the near-stream sites (L1 and R1) maintained a super-wet state on the  
 389 ground surface for a long time, which was beneficial for the production of CH<sub>4</sub>. However, the  
 390 wetlands maintained a state without water accumulation on the soil surface in August, which was  
 391 conducive to the oxidative absorption of CH<sub>4</sub>. SMC thus masked the effect of ST on CH<sub>4</sub>

392 emissions.

393 Previous studies indicated that temperature is an important factor affecting N<sub>2</sub>O emissions  
394 (Sun et al., 2011) through primary mechanisms impacting the nitrifying and denitrifying bacteria  
395 in the soil. Table 4 shows that the correlations between N<sub>2</sub>O emissions and ST10 and ST20 are  
396 poor ( $P > 0.05$ ). This can be attributed to the wide suitable temperature range for  
397 nitrification-denitrification and weak sensitivity to temperature. Malhi et al. (1982) found that the  
398 optimum temperature for nitrification was 20 °C, and it will inhibit entirely at 30 °C. However,  
399 Brady (1999) believed that the suitable temperature range for nitrification was 25~35°C, and the  
400 nitrification inhibits below 5 °C or above 50 °C. It showed that the temperature requirements of  
401 nitrifying microorganisms in wetland soils were different in different temperature belts. The  
402 suitable temperature range was the performance of the long-term adaptability of nitrifying  
403 microorganisms. Meanwhile, several studies revealed that denitrification could be carried out in a  
404 wide temperature range (5~70 °C), and it was positively related to temperature (Fan., 1995).  
405 However, the process will be inhibited when the temperature ~~is too high or too low~~. The average  
406 ST in wet season was 27.4°C, conducive to the growth of denitrifying microorganisms, while that  
407 in dry season was 8.97°C, and the microbial activity was generally low (Sun et al., 2011).  
408 Furthermore, ST fluctuations were low both in wet season and dry season. Therefore, the effect of  
409 ST on N<sub>2</sub>O emissions was masked by other factors, such as moisture content.

删除[liuxinyu]:

#### 410 4.1.3 Effects of BIO and soil organic matter on GHG emissions

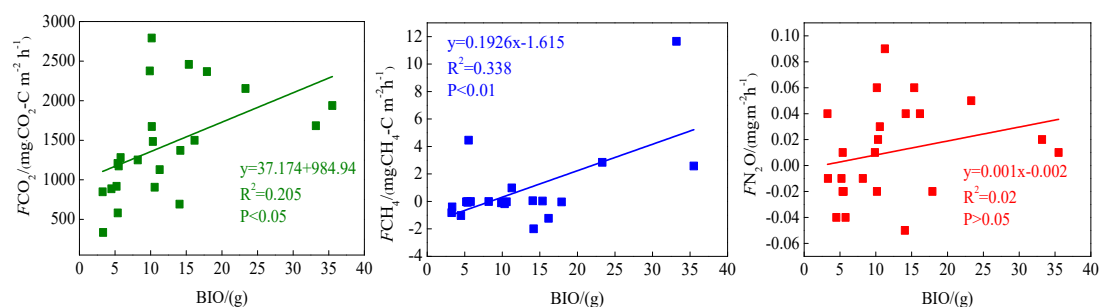
411 CO<sub>2</sub> and CH<sub>4</sub> emissions were higher in the riparian wetlands than in the grasslands, mainly  
412 because of greater vegetation cover. Typically, CO<sub>2</sub> emissions from riparian wetlands originate  
413 from plants and microorganisms, with plant respiration accounting for a large proportion in the  
414 growing season. Previous studies have shown that plant respiration accounts for 35–90% of the  
415 total respiration in the wetland ecosystem (Johnson-Randall and Foote, 2005). Good soil  
416 physicochemical properties and high soil total organic carbon (TOC) of riparian wetlands improve  
417 the activity of soil microorganisms and plant root respiration. Table 4 shows that BIO is  
418 significantly correlated with the CO<sub>2</sub> ( $P < 0.05$ ) and CH<sub>4</sub> ( $P < 0.01$ ) emissions. These results can  
419 be attributed to the significant linear positive correlation between the respiration rate and plant  
420 biomass (Lu et al., 2007). Higher plant biomass storage can achieve more carbon accumulation  
421 during photosynthesis and higher exudate release by the roots. This, in turn, promotes the

422 accumulation of soil organic matter. Increased amount of organic matter stimulates the growth and  
 423 reproduction of soil microorganisms, ultimately promoting CO<sub>2</sub> and CH<sub>4</sub> emissions. Moreover,  
 424 plants act as a gas channel for CH<sub>4</sub> transmission, and a larger amount of biomass promotes CH<sub>4</sub>  
 425 emissions, given the increased number of channels. In transect T3, high CO<sub>2</sub> emissions observed  
 426 at site L3 can be attributed to the relatively high levels of SMC, BIO, and soil nutrients, which  
 427 stimulate the microbial respiration rates.

428 BIO had a weak correlation with N<sub>2</sub>O emissions (Table 4), which indicates that plants  
 429 increase N<sub>2</sub>O production and emissions, although this may not be the most critical factor. Previous  
 430 studies reported mechanisms where in the plants can absorb N<sub>2</sub>O produced in the soil through the  
 431 root system before releasing it into the atmosphere. Additionally, the root exudates of plants can  
 432 enhance the activity of nitrifying and denitrifying bacteria in the soil, ultimately promoting the  
 433 production of N<sub>2</sub>O. Finally, oxygen stress caused by plant respiration can regulate the production  
 434 and consumption of N<sub>2</sub>O in the soil, eventually affecting the conversion of nitrogen in the soil  
 435 (Koops et al., 1996; Azam et al., 2005).

436 Site L3 in transect T3 was covered by tall reeds, and its BIO was much higher than those of  
 437 the other sites; thus, the data for this site were excluded from the correlation analysis.

438



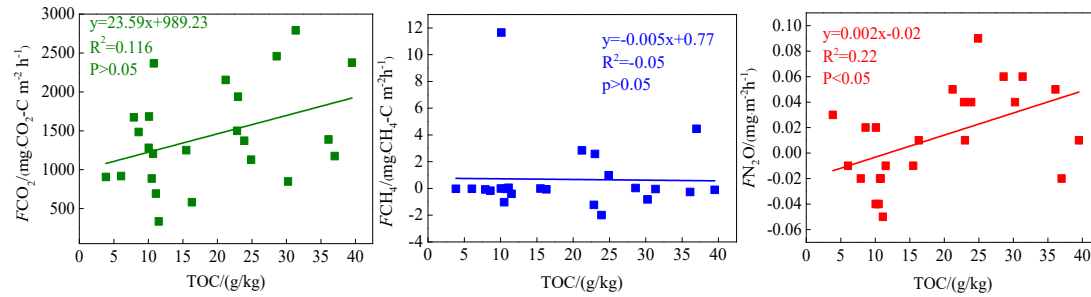
439

440 Fig. 7 Correlation between aboveground biomass (BIO) and GHG emissions (*F*)

441

442 Soil C:N ratio refers to the ratio of biodegradable carbonaceous organic matter and  
 443 nitrogenous matter in the soil, and it forms the soil matrix with TOC. TOC decomposition  
 444 provides energy for microbial activity, while the C:N ratio affects the decomposition of organic  
 445 matter by soil microorganisms (Gholz et al., 2010). The correlation results (Fig. 8) indicate that  
 446 TOC has a weak positive correlation with CO<sub>2</sub> emissions ( $P > 0.05$ ), but soil C:N has a significant

447 negative correlation with CO<sub>2</sub> emissions ( $P < 0.05$ ), indicating that nitrogen has a limiting effect  
448 on soil respiration by affecting microbial metabolism. Liu et al. (2019) reported that N addition  
449 promoted CO<sub>2</sub> emissions from wetlands soil, and the effect of organic N input was significantly  
450 higher than those of inorganic N input. Organic carbon provides a carbon source for the growth of  
451 plants and microorganisms, which boosts their respiration. Moreover, TOC has a significant  
452 correlation with N<sub>2</sub>O emissions ( $P < 0.05$ ). Most heterotrophic microorganisms use soil organic  
453 matter as carbon and electron donors (Morley N and Baggs E M., 2010). Soil carbon source has an  
454 important influence on microbial activity. Nitrifying or denitrifying microorganisms need organic  
455 matter to provide carbon source during the assimilation of NH<sub>3</sub> or NO<sub>3</sub><sup>-</sup>. The high content of  
456 organic matter in the soil can promote the abundance of heterotrophic nitrifying bacteria increases,  
457 consume dissolved oxygen in the medium, and cause the soil to become more anaerobic, slowing  
458 down autotrophic growth nitrifying bacteria. This reduces the nitrification rate, ultimately  
459 promoting N<sub>2</sub>O release. Enwall et al. (2005) studied the effect of long-term fertilization on soil  
460 denitrification microbial action intensity. They found that the soil with long-term organic fertilizer  
461 application has a significant increase in organic matter content, and consequently, a significant  
462 increase in denitrification activity. Typically, low soil C:N ratios are favorable for the  
463 decomposition of microorganisms, the most suitable range being between 10 and 12 (Pierzynski et  
464 al., 1994). Table 4 shows that N<sub>2</sub>O emissions are significantly related to the soil C:N ratios ( $P <$   
465  $0.05$ ), which means that denitrifying bacteria will use their endogenous carbon source for  
466 denitrification when the external carbon source is insufficient. Moreover, incomplete  
467 denitrification leads to the accumulation of NO<sub>2</sub>-N, which is conducive to the N<sub>2</sub>O release.  
468 Meanwhile, due to the weak competitive ability of Nos to electrons, low C:N inhibits the synthesis  
469 of Nos, which is also a reason for N<sub>2</sub>O release. In this study, all the sites in transects T1–T4  
470 exhibited similar soil C:N ratios in the optimum range (Table 1), which is favorable for microbial  
471 decomposition. However, the soil C:N ratios in transect T5 were higher than those in the other  
472 transects, especially in the dry lake bed. Therefore, transect T5 showed severe mineralization and  
473 a low microbial decomposition rate.  
474



475

476

Fig. 8 Correlations between soil organic carbon (TOC) and GHG emissions ( $F$ )

477

Table 4. Correlations between CO<sub>2</sub>, CH<sub>4</sub>, and N<sub>2</sub>O emissions and impact factors ( $n = 62$ )

GHG flux	ST10	ST20	SMC10	SMC20	TOC	$\rho_b$	C:N	pH	EC	BIO
CO <sub>2</sub>	0.634**	0.592**	0.307*	0.216	0.393	-0.463**	-0.289*	-0.350**	-0.251*	0.491*
CH <sub>4</sub>	-0.029	-0.051	0.346**	0.353**	-0.02	-0.129	-0.156	-0.127	-0.107	0.607**
N <sub>2</sub> O	0.127	0.118	0.304*	0.356**	0.493*	-0.194	0.311*	0.137	0.504**	0.251

478

Note: 1. The analysis method used in the table is Pearson correlation analysis, and the numbers

479

represent Pearson correlation coefficients.

480

2. \* and \*\* denote significant and highly significant correlations ( $P < 0.01$  and  $P < 0.05$ ),

481

respectively.

482

3. ST - soil temperature, SMC - soil moisture content,  $\rho_b$  - soil bulk density, soil C:N - soil

483

carbon-nitrogen ratio, pH - soil pH, EC - soil electrical conductivity, BIO - aboveground biomass

484

#### 4.2 Riparian wetlands as hotspots of GHG emissions

485

The results of this study emphasized that CO<sub>2</sub> emissions in the riparian wetlands were higher

486

than those in the hillslope grasslands owing to a variety of factors. ST is an important factor

487

affecting GHG emissions. Mclain and Martens (2006) showed that seasonal fluctuations in ST and

488

SMC in semi-arid regions have important effects on CO<sub>2</sub>, CH<sub>4</sub>, and N<sub>2</sub>O emissions in riparian

489

soils. Poblador et al. (2017) studied the GHG emissions in forest riparian zones and suggested that

490

the difference in the CO<sub>2</sub> and N<sub>2</sub>O emissions in these zones is affected by the spatial gradient of

491

the regional SMC. In this study, the upstream riparian wetlands are characterized by higher TOC,

492

lower soil C:N ratio, and abundant BIO than the hillslope grasslands (Table 1). These soil

493

conditions benefited the soil microbial activity, ultimately enhancing respiration as well as CO<sub>2</sub>

494

emissions. However, CO<sub>2</sub> emissions in downstream areas were nearly identical to those in the

495

grasslands because the wetlands gradually evolved into grasslands after their degradation. The

496 N<sub>2</sub>O emissions showed spatial patterns similar to those of the CO<sub>2</sub> emissions because the CO<sub>2</sub>  
497 concentrations were closely related to nitrification and denitrification processes. High CO<sub>2</sub>  
498 concentrations can promote the carbon and nitrogen cycles in soil (Azam et al., 2005), increasing  
499 below ground C allocation associated with increased root biomass, root turnover, and root  
500 exudation in elevated pCO<sub>2</sub> plants provided the energy for denitrification in the presence of high  
501 available N, or that there was increased O<sub>2</sub> consumption under elevated pCO<sub>2</sub> (Baggs et al., 2003).  
502 Moreover, soil respiration increases during soil denitrification (Liu et al., 2010; Christensen et al.,  
503 1990). In this study, a weak correlation was observed between the CO<sub>2</sub> and CH<sub>4</sub> emissions in the  
504 riparian zones ( $r = 0.228$ ), but CO<sub>2</sub> emissions were significantly correlated with N<sub>2</sub>O emissions ( $r$   
505  $= 0.322$ ,  $P < 0.05$ ). The soil became anaerobic in the riparian areas as the SMC increased, and this  
506 was conducive to the survival of CH<sub>4</sub>-producing bacteria and denitrification reactions, eventually  
507 leading to an increase in CH<sub>4</sub> and N<sub>2</sub>O emissions. Jacinthe et al. (2015) reported that inundated  
508 grassland-dominated riparian wetlands were CH<sub>4</sub> sinks ( $-1.08 \pm 0.22 \text{ kg} \cdot \text{CH}_4\text{-C ha}^{-1} \cdot \text{yr}^{-1}$ ), and Lu  
509 et al. (2015) also indicated that grasslands were CH<sub>4</sub> sinks. In our study, a marked water gradient  
510 across the transects led to the transformation of the soil from anaerobic to aerobic soil, which  
511 changed the wetland function as a CH<sub>4</sub> source or sink. Therefore, during the transition from the  
512 riparian wetlands to the hillslope grasslands, CH<sub>4</sub> emissions only appeared as sources in the  
513 near-stream sites and sinks at other sites.

514 Further, we compared the GHG emissions of riparian wetlands and hillslope grasslands  
515 around the Xilin River Basin with various types of grasslands (meadow grassland, typical  
516 grassland, and desert grassland) in the Xinlingol League in Inner Mongolia (Table 5). The CO<sub>2</sub>  
517 emissions in wet season decreased in the following order: upstream riparian wetlands >  
518 downstream riparian wetlands > hillslope grasslands > meadow grassland > typical grassland >  
519 desert grassland. Moreover, the upper riparian wetlands acted as source of CH<sub>4</sub> emissions, while  
520 the downstream transects and grasslands served as CH<sub>4</sub> sinks. Similarly, except for the  
521 downstream transects, N<sub>2</sub>O emissions occurred as weak sources in different types of grasslands  
522 and upstream riparian wetlands. The GHG emissions showed similar spatial patterns in October.  
523 Although these estimates were made only in the growing season in August and the non-growing  
524 season in October, our results suggest that riparian wetlands are the potential hotspots of GHG  
525 emissions. Thus, it is important to study GHG emissions to obtain a comprehensive picture of the

526 role of riparian wetlands in climate change.

527

528

Table 5. GHG emission fluxes of riparian wetlands and grasslands

Sample plot	GHG emissions in August ( $\text{mg}\cdot\text{m}^{-2}\cdot\text{h}^{-1}$ )			GHG emissions in October ( $\text{mg}\cdot\text{m}^{-2}\cdot\text{h}^{-1}$ )			Reference
	CO <sub>2</sub>	CH <sub>4</sub>	N <sub>2</sub> O	CO <sub>2</sub>	CH <sub>4</sub>	N <sub>2</sub> O	
Wetlands of upstream transects (T1, T2, and T3)	n=13 1606.28 ± 697.78	1.417 ± 3.41	0.031 ± 0.03	182.35 ± 88.26	0.272 ± 0.49	0.002 ± 0.005	
Wetlands of downstream transects (T4 and T5)	n=7 1144.15 ± 666.50	-0.215 ± 0.45	-0.037 ± 0.05	98.13 ± 15.11	-0.015 ± 0.05	0.001 ± 0.01	This study
Hillslope grasslands of all transects	n=7 1071.54 ± 225.39	-0.300 ± 0.40	0.003 ± 0.03	77.68 ± 25.32	-0.048 ± 0.03	-0.002 ± 0.005	
Meadow grassland	166.39 ± 45.89	-0.038 ± 0.009	0.002 ± 0.001	-	-	-	
Typical grassland	240.32 ± 87.56	-0.042 ± 0.025	0.037 ± 0.034	-	-	-	Guo et al., 2017
Desert grassland	107.59 ± 54.10	-0.036 ± 0.015	0.003 ± 0.001	-	-	-	
Typical grassland	520.25 ± 59.07	-0.102 ± 0.012	0.007 ± 0.001	88.34 ± 9.84	-0.099 ± 0.003	0.005 ± 0.001	Zhang, 2019
Typical grassland	232.42 ± 18.90	-0.090 ± 0.005	0.004 ± 0.001	-	-	-	
Typical grassland	265.23 ± 31.43	-0.185 ± 0.018	0.005 ± 0.001	189.41 ± 28.96	-0.092 ± 0.012	0.004 ± 0.001	Chao, 2019
Meadow grassland	553.85	-0.163	0.003	47.73	-0.019	0.011	
Typical grassland	308.60	-0.105	0.002	70.25	-0.029	0.007	Geng, 2004

529

530 We roughly estimated the annual cumulative emissions of CO<sub>2</sub>, CH<sub>4</sub>, and N<sub>2</sub>O from riparian  
531 wetlands and hillslope grasslands around the Xilin River Basin, and further calculated its global  
532 warming potential. Table 6 indicated that annual cumulative emissions of CO<sub>2</sub> and CH<sub>4</sub> decreased  
533 in the following order: upstream riparian wetlands > downstream riparian wetlands > hillslope  
534 grasslands, and N<sub>2</sub>O in the following order: upstream riparian wetlands > hillslope grasslands >  
535 downstream riparian wetlands. In this study, we used the static dark-box method to measure CO<sub>2</sub>

536 emissions, which does not consider the absorption and fixation of CO<sub>2</sub> by plants' photosynthesis.

537 Therefore, the total annual cumulative CO<sub>2</sub> emissions are high. ~~This result clearly showed that the~~

删除[liuxinyu]:

538 ~~significant impact of CO<sub>2</sub> emissions than CH<sub>4</sub> and N<sub>2</sub>O emissions on global warming.~~ The GWP

539 depends on the cumulative emissions of the GHGs. GWP is shown as (Table 6): upstream riparian

540 wetlands (13474.91 kg/hm<sup>2</sup>) > downstream riparian wetlands (8974.12 kg/hm<sup>2</sup>) > hillslope

541 grasslands (8351.24 kg/hm<sup>2</sup>). Therefore, both riparian wetlands and grasslands are the “sources”

542 of GHGs on a 100-year time scale. The source strength of wetlands is higher than grasslands,

543 further indicating that riparian wetlands are the hotspots of GHG emissions.

544

545 Table 6 Cumulative annual emission flux and global warming potential of GHGs in riparian  
546 wetlands and grasslands

Sample plot	CO <sub>2</sub> /kg/hm <sup>2</sup>	CH <sub>4</sub> /kg/hm <sup>2</sup>	N <sub>2</sub> O/kg/hm <sup>2</sup>	GWP/CO <sub>2</sub> kg hm <sup>2</sup>
Wetlands of upstream transects (T1, T2, and T3)	13092.8±5378.16	12.36±26.40	0.25±0.23	13474.91±5828.68
Wetlands of downstream transects (T4 and T5)	9093.47±4831.82	-1.68±3.23	-0.26±0.40	8974.12±4912.75
Hillslope grasslands of all transects	8412.26±1614.26	-2.55±3.12	0.01±0.20	8351.24±1648.22

547

#### 548 4.3 Effects of riparian wetland degradation on GHG emissions

549 The hydrology and soil properties showed ~~evident~~ differences among the transects because

删除[liuxinyu]:

550 the downstream zone was dry all year due to the presence of the Xilinhote Dam (Fig. 1). The dam

551 caused the degradation of the riparian wetlands, resulting in reduced GHG emissions. The average

552 CO<sub>2</sub> emissions amounted to 1663 mg·m<sup>-2</sup>·h<sup>-1</sup> in the riparian wetlands in the upstream transects

553 (T1, T2, and T3), while the downstream transects (T4 and T5) recorded an average of 1084

554 mg·m<sup>-2</sup>·h<sup>-1</sup>, 35% lower than the value in the upstream transects. The N<sub>2</sub>O emissions from the

555 riparian wetlands were lower in the downstream transects.

556 The wetland degradation first resulted in the continuous reduction of SMC, which led to the

557 deepening of the wetland's aerobic layer thickness. Besides, SMC could affect ST's change and

558 thus transformed CH<sub>4</sub> emissions from a source to a sink by affecting methanogens' activity (Yan et

559 al., 2018). Secondly, the reduction of SMC impeded aboveground plants' physiological activities

560 and inhabited related enzymes' activities in the respiration process. Meanwhile, various enzyme  
561 reactions of underground microorganisms under water stress influence and reduced CO<sub>2</sub> emissions  
562 (Zhang et al., 2017). Finally, after wetland degradation, long-term drought caused too low SMC,  
563 which was not conducive to the growth of nitrifying and denitrifying bacteria, which caused the  
564 transformation of N<sub>2</sub>O emissions from source to sink (Zhu et al., 2013). Table 1 shows that soil  
565 TOC in the upstream transects (average: 25.1 g·kg<sup>-1</sup>) is higher than that in the downstream  
566 transects (average: 8.41 g·kg<sup>-1</sup>). The relatively low SMC and the aerobic environment were  
567 conducive to the mineralization and decomposition of TOC. The degradation of plants in the  
568 wetlands led to the gradual reduction of BIO. Ultimately, the plant carbon source input of the  
569 degraded wetlands decreased, and the bare land temperature increased due to the reduced plant  
570 shelter. This accelerated the decomposition of TOC, leading to its decrease. This result indicates  
571 that wetland degradation caused the soil carbon pool's loss and weakened the wetland carbon  
572 source/sink function. These results are in agreement with those of Xia (2017).

573 The degraded wetlands also caused soil desertification and salinization, leading to a decline  
574 in the physical protection afforded by organic carbon and a reduction in soil aggregates. Thus, the  
575 preservation provided by organic carbon declined. TOC and SMC in the dry lake bed in transect  
576 T5 were relatively high, but GHG emissions were very low along this transect because soil pH  
577 values increased after the degradation of the lake soil, exceeding the optimum range required for  
578 microorganism activity. The soil C:N ratio was very high, resulting in severe mineralization and a  
579 low microbial decomposition rate, hence affecting the GHG emissions.

580

## 581 **5. Conclusions**

582 The riparian wetlands in the Xilin River Basin constitute a dynamic ecosystem. The present  
583 spatial and temporal transfers in the studied biogeochemical processes were attributed to the  
584 changes in SMC, ST, and soil substrate availability. Our simultaneous analysis of CO<sub>2</sub>, CH<sub>4</sub>, and  
585 N<sub>2</sub>O emissions from riparian wetlands and hillslope grasslands in the Xilin River Basin revealed  
586 that the majority of the GHG emissions occurred in the form of CO<sub>2</sub>. Moreover, our results clearly  
587 illustrated a marked seasonality and spatial pattern of GHG emissions along the transects and in  
588 the longitudinal direction (i.e., upstream and downstream). SMC and ST were two critical factors

589 controlling the GHG emissions. Moreover, abundant BIO promoted the CO<sub>2</sub>, CH<sub>4</sub>, and N<sub>2</sub>O  
590 emissions.

591 The riparian wetlands were the potential hotspots of GHG emissions in the Inner Mongolian  
592 region. However, the degradation of wetlands transformed the area from a source to a sink for CH<sub>4</sub>  
593 and N<sub>2</sub>O emissions, and reduced CO<sub>2</sub> emissions, which severely affected the wetland carbon cycle  
594 processes. **Our results show that the riparian wetlands have high CO<sub>2</sub> emissions, but wetlands are**  
595 **CO<sub>2</sub> sink in the overall CO<sub>2</sub> balance general due to the photosynthesis of plants.** Overall, our study  
596 suggests that anthropogenic activities have significantly changed the hydrological characteristics  
597 of the studied area, and will accelerate carbon loss from the riparian wetlands and further  
598 influence the GHG emissions in the future.

### 599 **Author Contributions**

600 Xinyu Liu, Xixi Lu and Ruihong Yu designed the research framework and wrote the  
601 manuscript. Xixi Lu and Ruihong Yu supervised the study. Xinyu Liu, Hao Xue, Zhen Qi,  
602 Zhengxu Cao and Zhuangzhuang Zhang carried out the field experiments and laboratory  
603 experiments analyses. Z.Z. drew GIS mapping in this paper. Tingxi Liu proofread the manuscript.  
604 **Heyang Sun contributed much in the revised version of our manuscript.**

### 605 **Acknowledgements**

606 **This study was funded by the National Key Research and Development Program of China**  
607 **(grant no. 2016YFC0500508), Major Science and Technology Projects of Inner Mongolia**  
608 **Autonomous Region (grant nos. 2020ZD0009 and ZDZX2018054), National Natural Science**  
609 **Foundation of China (grant no. 51869014), Key Scientific and Technological Project of Inner**  
610 **Mongolia (grant no. 2019GG019), and Open Project Program of the Ministry of Education Key**  
611 **Laboratory of Ecology and Resources Use of the Mongolian Plateau (grant no. KF2020006).**

### 612 **Competing interests**

613 The authors declare no conflicts of interest.

### 614 **References**

615 Azam F., Gill S., Farooq S.: Availability of CO<sub>2</sub> as a factor affecting the rate of nitrification in soil,  
616 Soil Biology & Biochemistry, 37, 2141–2144, doi 10.1016/j.soilbio.2005.02.036, 2005.  
617 Baggs E.M., Richter M., Cadisch G., Hartwig U.A.: Denitrification in grass swards is increased  
618 under elevated atmospheric CO<sub>2</sub>, Soil Biology and Biochemistry, 35, 729–732, doi

619 10.1016/S0038-0717(03)00083-X, 2003.

620 Beger M., Grantham H.S., Pressey R.L., Wilson K.A., Peterson E.L., Dorfman D., Lourival R.,  
621 Brumbaugh D.R., Possingham H.P.: Conservation planning for connectivity across marine,  
622 freshwater, and terrestrial realms, *Biological Conservation*, 143, 565–575, doi  
623 10.1016/j.biocon.2009.11.006, 2010.

624 Brady N C.: *Nature and properties of soils*, New Jersey: Prentice-Hall, Inc., doi 10.2307/3894608,  
625 1999.

626 Cao M., Yu G., Liu J., Li K.; Multi-scale observation and cross-scale mechanistic modelling on  
627 terrestrial ecosystem carbon cycle, *Science in China Ser. D Earth Sciences*, 48, 17–32, doi  
628 10.1360/05zd0002, 2005.

629 Chao R.: *Effects of Simulated Climate Change on Greenhouse Gas Fluxes in Typical Steppe*  
630 *Ecosystem*, Inner Mongolia University, 2019.

631 Cheng S and Huang J.: Enhanced soil moisture drying in transitional regions under a warming  
632 climate, *Journal of Geophysical Research-Atmospheres*, 121, 2542–2555, doi  
633 10.1002/2015JD024559, 2016.

634 Christensen S., Simkins S., Tiedje J M.: Temporal Patterns of Soil Denitrification: Their Stability  
635 and Causes, *Soil Science Society of America Journal*, 54, 1614, doi  
636 10.2136/sssaj1990.03615995005400060017x, 1990.

637 Ding W., Cai Z., Tsuruta H.: Cultivation, nitrogen fertilization, and set - aside effects on methane  
638 uptake in a drained marsh soil in Northeast China, *Global Change Biology*, 10, 1801 – 1809, doi  
639 10.1111/j.1365-2486.2004.00843.x, 2010.

640 Enwall K., Philippot L., Hallin S.: Activity and composition of the denitrifying bacterial  
641 community respond differently to long-term fertilization, *Applied and Environmental*  
642 *Microbiology*, 71, 8335-8343, doi 10.1128/AEM.71.12.8335-8343.2005, 2005.

643 Fan X.: *Research on nitrification potential and denitrification potential of soil in several farmland*  
644 *in China*, Nanjing Institute of Soil Sciences, Chinese Academy of Sciences, 1995.

645 Ferrón S., Ortega T., Gómez-Parra A., Forja J.M.: Seasonal study of dissolved CH<sub>4</sub>, CO<sub>2</sub> and N<sub>2</sub>O  
646 in a shallow tidal system of the bay of Cádiz (SW Spain), *Journal of Marine Systems*, 66, 244–257,  
647 doi 10.1016/j.jmarsys.2006.03.021, 2007.

648 Geng H.: *Study on Characters of CO<sub>2</sub>, CH<sub>4</sub>, N<sub>2</sub>O Fluxes and the Relationship between Them and*

649 Environmental Factors in the Temperate Typical Grassland Ecosystem, Northwest Agriculture &  
650 Forestry University, 2004.

651 Gholz H.L., Wedin D.A., Smitherman S.M., Harmon M.E., Parton W.J.: Long-term dynamics of  
652 pine and hardwood litter in contrasting environments: toward a global model of decomposition,  
653 *Global Change Biology*, 6, 751–765, doi 10.1046/j.1365-2486.2000.00349.x, 2000.

654 Gou Q., Qu J., Wang G., Xiao J., Pang Y.: Progress of wetland researches in arid and  
655 semi-arid regions in China, *Arid Zone Research*, 1001–4675, 213–220, 2015.

656 Guo X., Zhou D., Li Y.: Net Greenhouse Gas Emission and Its Influencing Factors in Inner  
657 Mongolia Grassland, Chinese Grassland Society, 2017.

658 Heilman J.L., Cobos D.R., Heinsch F.A., Campbell C.S., McInnes K.J.: Tower-based conditional  
659 sampling for measuring ecosystem-scale carbon dioxide exchange in coastal wetlands, *Estuaries*,  
660 22, 584–591, doi 10.2307/1353046, 1999.

661 Inubushi K., Furukawa Y., Hadi A., Purnomo E., Tsuruta H.: Seasonal changes of CO<sub>2</sub>, CH<sub>4</sub> and  
662 N<sub>2</sub>O fluxes in relation to land-use change in tropical peatlands located in coastal area of South  
663 Kalimantan, *Chemosphere*, 52, 603–608, doi 10.1016/s0045-6535(03)00242-x, 2003.

664 IPCC.: Climate Change 2013: The Physical Science Basis. Contribution of Working, Working  
665 Group I of the IPCC, 43, 866–871, 2013.

666 Jacinthe P.A., Vidon P., Fisher K., Liu X., Baker M.E.: Soil Methane and Carbon Dioxide Fluxes  
667 from Cropland and Riparian Buffers in Different Hydrogeomorphic Settings, *Journal of*  
668 *Environment Quality*, 44, 1080–1115, doi 10.2134/jeq2015.01.0014, 2015.

669 Johnson-Randall L.A., Foote A.L.: Effects of managed impoundments and herbivory on wetland  
670 plant production and stand structure, *Wetlands*, 25, 38–50, doi  
671 10.1672/0277-5212(2005)025[0038:eomiah]2.0.co;2, 2005.

672 Koops J.G., Oenema O., Beusichem M.L.: Denitrification in the top and sub soil of grassland on  
673 peat soils, *Plant and Soil*, 184, 1–10, doi 10.1007/bf00029269, 1996.

674 Kou X.: Study on Soil Physicochemical Properties and Bacterial Community Characteristics of  
675 River Riparian Wetland in Inner Mongolia Grassland, Inner Mongolia University, 2018.

676 Liu C.: Effects of Nitrogen Addition on the CO<sub>2</sub> Emissions in the Reed (*Phragmites australis*)  
677 Wetland of the Yellow River Delta, China, Liaocheng University, 2019.

678 Liu C., Xie G., Huang H.: Shrinking and drying up of Baiyangdian Lake wetland: a natural or

679 human cause? *Chinese Geographical Science*, 16, 314–319, 2006.

680 Liu F., Liu C., Wang S., Zhu Z.: Correlations among CO<sub>2</sub>, CH<sub>4</sub>, and N<sub>2</sub>O concentrations in soil  
681 profiles in central Guizhou Karst area, *Chinese Journal of Ecology*, 29, 717–723, doi  
682 10.1016/S1872-5813(11)60001-7, 2010.

683 Liu J., Wang J., Li Z., Yu J., Zhang X., Wang C., Wang Y.: N<sub>2</sub>O Concentration and Its Emission  
684 Characteristics in Sanjiang Plain Wetland, *Chinese Journal of Environmental Science*, 24, 33–39,  
685 2003.

686 Lu Y., Song C., Wang Y., Zhao Z.: Influence of plants on CO<sub>2</sub> and CH<sub>4</sub> emission in wetland  
687 ecosystem, *Acta Botanica Boreali-Occidentalia Sinica*, 27, 2306–2313, 2007.

688 Lu Z., Du R., Du P., Li Z., Liang Z., Wang Y., Qin S., Zhong L.: Effect of mowing on N<sub>2</sub>O and  
689 CH<sub>4</sub> fluxes emissions from the meadow-steppe grasslands of Inner Mongolia, *Frontiers of Earth  
690 Science*, 9, 473–486, doi 10.1007/s11707-014-0486-z, 2015.

691 Lv M., Sheng L., Zhang L.: A review on carbon fluxes for typical wetlands in different climates of  
692 China, *Wetland Science*, 11, 114–120, doi CNKI:SUN:KXSD.0.2013-01-020, 2013.

693 Malhl S.S., Mcgill W.B.: Nitrification in three Alberta soils: effects of temperature, moisture and  
694 substrates concentration, *Soil Biology and Biochemistry*, 14, 393–399, doi  
695 10.1016/0038-0717(82)90011-6 1982.

696 Mclain J E T., Martens D.A.: Moisture controls on trace gas fluxes in semiarid riparian soils, *Soil  
697 Science Society of America Journal*, 70, 367, doi 10.2136/sssaj2005.0105, 2006.

698 Meng W., Wu D., Wang Z.: Control factors and critical conditions between carbon sinking and  
699 sourcing of wetland ecosystem, *Ecology and Environmental Sciences*, 20, 1359–1366, doi  
700 10.1016/S1671-2927(11)60313-1, 2011.

701 Mitsch W.J., Gosselink J.G.: *Wetlands (Fourth Edition)*, John Wiley & Sons Inc.: Hoboken, New  
702 Jersey, USA, 2007.

703 Mitsch W.J., Gosselink J.G., Anderson C.J., Anderson, C. J.: *Wetland ecosystems*: John Wiley &  
704 Sons, 2009.

705 Moldrup P., Olesen T., Schjønning P., Yamaguchi T., Rolston D.E.: Predicting the gas diffusion  
706 coefficient in undisturbed soil from soil water characteristics, *Soil Science Society of America  
707 Journal*, 64, 1588–1594, doi 10.2136/sssaj2000.64194x, 2000.

708 Morley N., Baggs E.M.: Carbon and oxygen controls on N<sub>2</sub>O and N<sub>2</sub> production during nitrate

709 reduction, *Soil Biology & Biochemistry*, 42, 1864-1871, doi 10.1016/j.soilbio.2010.07.008, 2010.

710 Naiman R.J., Decamps H.: The ecology of interfaces: Riparian zones, *Annual Review of Ecology*  
711 & Systematics, 28, 621–658, doi 10.2307/2952507, 1997.

712 National Agricultural Technology Extension Service Center (NATESC):. Technical specification  
713 for soil analysis, 2006.

714 Niu C., Wang S., Guo Y., Liu W., Zhang J.: Studies on variation characteristics of soil nitrogen  
715 forms, nitrous oxide emission and nitrogen storage of the *Phragmites australis*-dominated  
716 land/inland water ecotones in Baiyangdian wetland, *Journal of Agricultural University of Hebei*,  
717 40, 72–79, 2017.

718 Pierzynski G M S., J.T., Vance, G.F.: *Soils and Environmental Quality*, 1994.

719 Poblador S., Lupon A., Sabaté S., Sabater F.: Soil water content drives spatiotemporal patterns of  
720 CO<sub>2</sub> and N<sub>2</sub>O emissions from a Mediterranean riparian forest soil, *Biogeosciences Discussions*, 14,  
721 1–28, doi 10.5194/bg-14-4195-2017, 2017.

722 Qin S., Tang J., Pu J., Xu Y., Dong P., Jiao L., Guo J.: Fluxes and influencing factors of CO<sub>2</sub> and  
723 CH<sub>4</sub> in Hangzhou Xixi Wetland, China, *Earth and Environment*, 44, 513–519, 2016.

724 Sjögersten S., Wal R V.D., Woodin S.J.: Small-scale hydrological variation determines landscape  
725 CO<sub>2</sub> fluxes in the high Arctic, *Biogeochemistry*, 80, 205–216, doi 10.2307/20456398, 2006.

726 Sun Y., Wu H., Wang Y.: The influence factors on N<sub>2</sub>O emissions from nitrification and  
727 denitrification reaction, *Ecology and Environmental Sciences*, 20, 384–388, doi  
728 10.1631/jzus.B1000275, 2011.

729 Tong C., Wu J., Yong S., Yang J., Yong W.: A landscape-scale assessment of steppe degradation in  
730 the Xilin River Basin, Inner Mongolia, China, *Journal of Arid Environments*, 59, 133–149, doi  
731 10.1016/j.jaridenv.2004.01.004, 2004.

732 Ulrike R., Jürgen A., Rolf R., Wolfgang M.: Nitrate removal from drained and reflooded fen soils  
733 affected by soil N transformation processes and plant uptake, *Soil Biology and Biochemistry*, 36,  
734 77-90, doi 10.1016/j.soilbio.2003.08.021, 2004.

735 Waddington J.M., Roulet N.T.: Carbon balance of a boreal patterned peatland, *Global Change*  
736 *Biology*, 6, 87–97, doi 10.1046/j.1365-2486.2000.00283.x, 2000.

737 Whiting G.J., Chanton J.P.: Greenhouse carbon balance of wetlands: methane emission versus  
738 carbon sequestration, *Tellus B*, 53, 521-528, doi 10.3402/tellusb.v53i5.16628, 2001.

739 WMO.: WMO Statement on the State of the Global Climate in 2017, World Meteorological  
740 Organization, 2018.

741 Xi X., Zhu Z., Hao X.: Spatial variability of soil organic carbon in Xilin River Basin, Research of  
742 Soil and Water Conservation, 24, 97–104, 2017.

743 Xia P., Yu L., Kou Y., Deng H., Liu J.: Distribution characteristics of soil organic carbon and its  
744 relationship with enzyme activity in the Caohai wetland of the Guizhou Plateau, Acta Scientiae  
745 Circumstantial, 37, 1479–1485, doi 10.13671/j.hjkxxb.2016.0129, 2017.

746 Xu H., Cai Z., Yagi K.: Methane Production Potentials of Rice Paddy Soils and Its Affecting  
747 Factors, Acta Pedologica Sinica, 45, 98–104, doi 10.1163/156939308783122788, 2008.

748 Yan L., Zhang X., Wang J., Li Y., Wu H., Kang X.: Drainage effects on carbon flux and carbon  
749 storage in swamps, marshes, and peatlands, Chin J Appl Environ Biol, 24, 1023–1031, doi  
750 10.19675/j.cnki.1006-687x.2017.11031, 2018.

751 Yu P., Zhang J., Lin C.: Progress of influence factors on N<sub>2</sub>O emission in farmland soil,  
752 Environment and sustainable development, 20–22, 2006.

753 Zhang D.: Effects of Different Grazing Intensities on Greenhouse Gases Flux in Typical Steppe of  
754 Inner Mongolia, Inner Mongolia University, 2019.

755 Zhang Y., Hao Y., Cui L., Li W., Zhang X., Zhang M., Li L., Yang S., Kang X.: Effects of extreme  
756 drought on CO<sub>2</sub> fluxes of Zoige alpine peatland, Journal of University of Chinese Academy of  
757 Sciences, 34, 462-470, 2017.

758 Zhang Z., Hua L., Yin X., Hua L., Gao J.: Nitrous oxide emission from agricultural soil land some  
759 influence factors, Journal of Capital Normal University: Natural Science Edition, 26, 114–120,  
760 2005.

761 Zhu X., Song C., Guo Y., Shi F., Wang L.: N<sub>2</sub>O emissions and its controlling factors from the  
762 peatlands in the Sanjiang Plain, China Environmental Sciences, 33, 2228 - 2234, 2013.

763 Zona D., Oechel W.C., Kochendorfer J., Paw U K.T., Salyuk A.N., Olivas P.C., Oberbauer S.F.,  
764 Lipson D.A.: Methane fluxes during the initiation of a large-scale water table manipulation  
765 experiment in the Alaskan Arctic tundra, Global Biogeochem Cycles, 23, doi  
766 10.1029/2009gb003487, 2009.